

1-D LOCAL CRUSTAL STRUCTURES FROM SEISMOLOGICAL DATA
IN THE CYPRUS SUBDUCTION ZONE AND ANTALYA BAY

by

Şükran Perk

B.Sc., Geophysical Engineering, Istanbul University, 2008

Submitted to the Kandilli Observatory and
Earthquake Research Institute in partial fulfillment of
the requirements for the degree of
Master of Science

Graduate Program in Geophysics Department

Boğaziçi University

2013

ACKNOWLEDGEMENTS

First of all, I wish to express my sincere thanks to my advisor Prof. Hayrullah Karabulut for the valuable support and guidance. His encouragement has significantly helped me in successful completion of my research. I would also like to express my appreciation to him for providing the opportunity for me to work with the subject I am truly interested in.

I wish to express my appreciation to Ali Deęer Özbakır for providing helpful discussion and information. I would also like to thank Ahu Kōmeç Mutlu for her helpful assistance during my thesis.

Thanks to the Kandilli Observatory and Earthquake Research Institute (KOERI), The Scientific and Technological Research Council of Turkey Marmara Research Center (TUBITAK-MAM), Prime Ministry Disaster and Emergency Management Presidency (AFAD) for providing seismic data.

I would like to thank my friends for their moral support and fun times. Thanks to my family for their love, care and support over many years.

ABSTRACT

1-D LOCAL CRUSTAL STRUCTURES FROM SEISMOLOGICAL DATA IN THE CYPRUS SUBDUCTION ZONE AND ANTALYA BAY

The eastern Mediterranean is a tectonically complex region, where long-term subduction and accretion processes have shaped the overall evolution. Recently, many seismic tomography studies have shown subducted slabs of the Neo-Tethyan lithosphere, continuing its subduction in the Hellenic trench, stalled in the Cyprus trench and being torn near the intersection between them. Antalya bay is a key region located on the western flank of the Cyprus Subduction Zone (CSZ), close to the junction between the Hellenic and Cyprus Arcs. Here deep earthquakes are nucleated, which otherwise cannot be seen anywhere else along the CSZ. For this reason, we focus our attention specifically to the Antalya Bay area but also the remaining parts of the CSZ. Several regional studies have been carried out to define the velocity structure beneath the region but none have been able to locate the CSZ. One of the main reasons for this was the lack of incorporation of a wide seismic network in those regional studies. We compile a large catalog of seismicity and relocate earthquakes to infer 1D local crustal structure using the clusters of seismicity.

We used seismic data between 2005 – 2011 which are recorded at more than 250 seismic stations operated by several agencies and portable deployments. The data-set is composed of over 10,000 events and earthquakes can be grouped in several distinct clusters. We defined five of these clusters, where the total number of events is more than 4500, among which we selected over 2000 events with the highest data quality. 1-D local P-wave velocity models are developed using this high quality data-set and the earthquakes are relocated using the local velocity models.

The compiled and reanalyzed data will contribute to perform local earthquake tomography. Moreover, obtained local velocity models represent a fundamental step towards an improved seismic tomography studies in a very crucial region in the eastern Mediterranean.

ÖZET

DEPREM VERİLERİ KULLANILARAK KIBRIS DALMA BATMA ZONU VE ANTALYA KÖRFEZİNDE BİR BOYUTLU KABUK YAPILARININ BULUNMASI

Doğu Akdeniz, uzun süreli yitim ve yığışım süreçlerinin şekillendirdiği tektonik olarak karmaşık bir bölgedir. Son yıllardaki sismik tomografi çalışmaları, Helenik trencinde yitimi devam eden, Kıbrıs trenç bölgesinde durmuş ve iki bölgenin arasında kopmaya başlamış Neo-Tetis litosferinin dalan kolunu göstermektedir. Antalya körfezi, Helenik ve Kıbrıs yayını birleştiren Kıbrıs dalma batma zonunun (KDBZ) batı kanadında bulunan önemli bir bölgedir. Bu bölgede KDBZ boyunca diğer bölgelerde görülmeyen derin depremler olmaktadır. Bu nedenle, özel olarak dikkatimizi Antalya körfezi çekse de KDBZ' nun diğer kısımları da incelenmiştir. Bölgedeki hız yapısını araştırmak için çeşitli çalışmalar yapılsa da hiç biri KDBZ'nu yerini tam olarak belirleyememiştir. Bunun temel nedenlerinden biri, bu çalışmalarda geniş bir sismik ağı kullanılmamış olmasıdır. Bu çalışmada, sismisite kullanılarak, bölgenin 1B kabuk yapısını elde etmek amacıyla geniş bir katalog hazırlanıp, bölgedeki depremlerin lokasyonları yeniden yapılmıştır.

2005-2011 yılları arasında çeşitli kurum ve projelerden sağlanan 250'den fazla sismik istasyonda kaydedilen sismik veri kullanılmıştır. Veri seti 10.000'den fazla depremi içerir ve depremler beş farklı küme halinde gruplandırılabilir. Bu kümelerdeki depremlerin toplam sayısı 4500' den fazla olup, en kaliteli 2000'den fazla deprem seçilmiştir. Bu data seti kullanılarak 1B P dalga hız modelleri geliştirilmiştir ve bu modeller kullanılarak depremlerin lokasyonu yeniden yapılmıştır.

Derlenen ve analizi yapılan veri bölgenin yerel deprem tomografisinin oluşturulmasına katkı sağlayacaktır. Ayrıca, elde edilen yerel hız modelleri, Doğu Akdeniz'de sismik tomografi çalışmalarına yönelik temel bir adımı temsil eder.

TABLE OF CONTENTS

ACKNOWLEDGEMENTS.....	iii
ABSTRACT	iv
ÖZET	v
TABLE OF CONTENTS	vi
LIST OF FIGURES	viii
LIST OF SYMBOLS	xi
LIST OF ACRONYMS/ABBREVIATIONS	xii
1. INTRODUCTION	1
1.1. Geology and Tectonic Settings	4
1.2. Seismotectonics of the study area.....	6
1.3. Previous Studies	8
2. METHOD.....	11
3. DATA PROCESSING.....	14
4. RESULTS.....	22
4.1. Region A: Fethiye	22
4.1.1. Hypocentral Locations	22
4.1.2. Station Corrections	23
4.1.3. Velocity Model.....	24
4.1.4. Statistical Properties	27
4.2. Region B: Adana	28
4.2.1. Hypocentral Locations	28
4.2.2. Station Corrections	29
4.2.3. Velocity Model	30
4.2.4. Statistical Properties	32
4.3. Region C: Konya	33
4.3.1. Hypocentral Locations	33
4.3.2. Station Corrections	34
4.3.3. Velocity Model.....	35
4.3.4. Statistical Properties	37
4.4. Region D: Cyprus	38
4.4.1. Hypocentral Locations	38

4.4.2. Station Corrections	39
4.4.3. Velocity Model.....	40
4.4.4. Statistical Properties	42
4.5. Region E: Antalya	43
4.5.1. Hypocentral Locations	43
4.5.2. Station Corrections	44
4.5.3. Velocity Model.....	45
4.5.4. Statistical Properties	47
4.6. Overall Velocity Profiles.	48
5. DISCUSSIONS.....	54
6. CONCLUSIONS.....	56
REFERENCES.....	57

LIST OF FIGURES

Figure 1.1. The map of the Eastern Mediterranean	2
Figure 1.2. Geological map of the Eastern Mediterranean	6
Figure 1.3. Focal mechanism solutions of the study area.....	8
Figure 3.1. Diagram of the inversion procedure for the computation of the 1D Minimum velocity model	14
Figure 3.2. Travel time arrivals of P and S phases	16
Figure 3.3. Reduced travel time arrivals of P and S phases	17
Figure 3.4. List of stations, which are used to analyze earthquakes in this study	18
Figure 3.5. Seismicity of southern Turkey between 2005-2011	19
Figure 3.6. The statistics of the initial catalog with the locations computed using the 1D velocity model and no station correction	20
Figure 3.7. The number of observations for each station	21
Figure 4.1. Relocated earthquakes for sub-region A	23
Figure 4.2. Station corrections of the earthquake cluster in sub-region A	24
Figure 4.3. P and S wave initial velocity models of the earthquake cluster in sub-region A.....	25
Figure 4.4. P and S wave velocity model of the earthquake cluster in sub-region A	26
Figure 4.5. Statistics of the catalog for the earthquake cluster in sub-region A.....	27
Figure 4.6. Relocated earthquakes for sub-region B	28
Figure 4.7. Station corrections of the earthquake cluster in sub-region B	29

Figure 4.8. P and S wave initial velocity models of the earthquake cluster in sub-region B.....	30
Figure 4.9. P and S wave velocity model of the earthquake cluster in sub-region B	31
Figure 4.10. Statistics of the catalog for the earthquake cluster in sub-region B.....	32
Figure 4.11. Relocated earthquakes for sub-region C	33
Figure 4.12. Station corrections of the earthquake cluster in sub-region C	34
Figure 4.13. P and S wave initial velocity models of the earthquake cluster in sub-region C.....	35
Figure 4.14. P and S wave velocity model of the earthquake cluster in sub-region C	36
Figure 4.15. Statistics of the catalog for the earthquake cluster in sub-region C.....	37
Figure 4.16. Relocated earthquakes for sub-region D	38
Figure 4.17. Station corrections of the earthquake cluster in sub-region D	39
Figure 4.18. P and S wave initial velocity models of the earthquake cluster in sub-region D.....	40
Figure 4.19. P and S wave velocity model of the earthquake cluster in sub-region D	41
Figure 4.20. Statistics of the catalog for the earthquake cluster in sub-region D.....	42
Figure 4.21. Relocated earthquakes for sub-region E	43
Figure 4.22. Station corrections of the earthquake cluster in sub-region E	44
Figure 4.23. P and S wave initial velocity models of the earthquake cluster in sub-region E.....	45
Figure 4.24. P and S wave velocity model of the earthquake cluster in sub-region E	46
Figure 4.25. Statistics of the catalog for the earthquake cluster in sub-region E.....	47
Figure 4.26. Final P and S velocity models for each cluster	48

Figure 4.27. Station corrections for all regions.....	49
Figure 4.28. The statistics of the catalog with the locations computed using the 1D velocity models estimated from the VELEST	50
Figure 4.29. Earthquakes which is relocated with 1-D velocity models and station corrections	51
Figure 4.30. Cross-section views of earthquake hypocenters	52

LIST OF SYMBOLS

t_{ij}	The body wave arrival time
u	The slowness field
t_{ij}^{calc}	Theoretical arrival times
t_{ij}^{obs}	Observed travel times
t_{ij}^{res}	Residual travel time
x_0	Latitude
y_0	Longitude
z_0	Depth
h	Vector of hypocentral parameter adjustments
m	Vector of model parameter adjustments
e	Vector of travel time errors
A	Matrix of all partial derivatives
d	Vector of hypocentral and model parameter adjustments

LIST OF ACRONYMS/ABBREVIATIONS

AB	Antalya Basin
ADB	Adana Basin
AFAD	Prime Ministry Disaster and Emergency Management Presidency
CB	<i>Cilicia Basin</i>
CSZ	Cyprus Subduction Zone
CYP	Cyprus
EAF	East Anatolian Fault
ES	Eratosthenes Seamount
FR	Florence Rise
GPS	Global Positioning System
KOERI	Kandilli Observatory and Earthquake Research Institute
LB	Levant Basin
RMS	Root Mean Square
TUBITAK-MAM	The Scientific and Technological research council of Turkey Marmara Research Center

1. INTRODUCTION

The Eastern Mediterranean region is a tectonically complex area where progressive Arabian-Eurasian convergence (McQuarrie *et al.*, 2003) led to the Afro-Eurasian collision (Şengör *et al.*, 2008). Whereas in the west, back-arc spreading due to the roll-back of the Hellenic trench is continuously producing the Aegean domain, related to the development of the Alpine orogenic belt (Dewey *et al.*, 1989; Wortel and Spakman, 2000; Jolivet and Faccenna, 2000 for a brief review). The Cyprus subduction zone lies in between these two end-member tectonic settings, i.e. Collision and back-arc extension, there lies its significance.

The present day processes and the evolution of an orogenic belt leave their marks on the crustal structure by the way of accretion, sedimentation, thinning and/or thickening of the crust. Therefore, we can decipher the crustal evolution by examining the crustal structure. Several studies have been performed to construct the crustal structure beneath the region, among which seismic tomography (Spakman, 1991; Piromallo and Morelli, 2003; Koulakov and Sobolev, 2006; Biryol *et al.*, 2011) and seismic refraction methods (Makris *et al.*, 1983; Ben-Avraham *et al.*, 2002; Netzeband *et al.*, 2006) have been employed. Nevertheless, there is still inadequate information on the crustal structure, its nature, the Moho depth and topography. We aim to infer 1D local crustal structures in the island of Cyprus and its vicinity, the Antalya Bay, Adana Basin, Konya and Fethiye region.

Figure 1.1 shows the topography, bathymetry and the main on-shore faults in the eastern Mediterranean region. There are also three labels on the map which is outside of the study regions. We mention briefly about them because they play an important role in regional tectonics. The Florence Rise extends from the island of Cyprus in the southwest to Antalya Basin. The Levant Basin is located at the eastern part of the Eastern Mediterranean. It is a small basin enclosed by continental masses. The northeastern Mediterranean is dominated by Adana and Cilicia Basins.

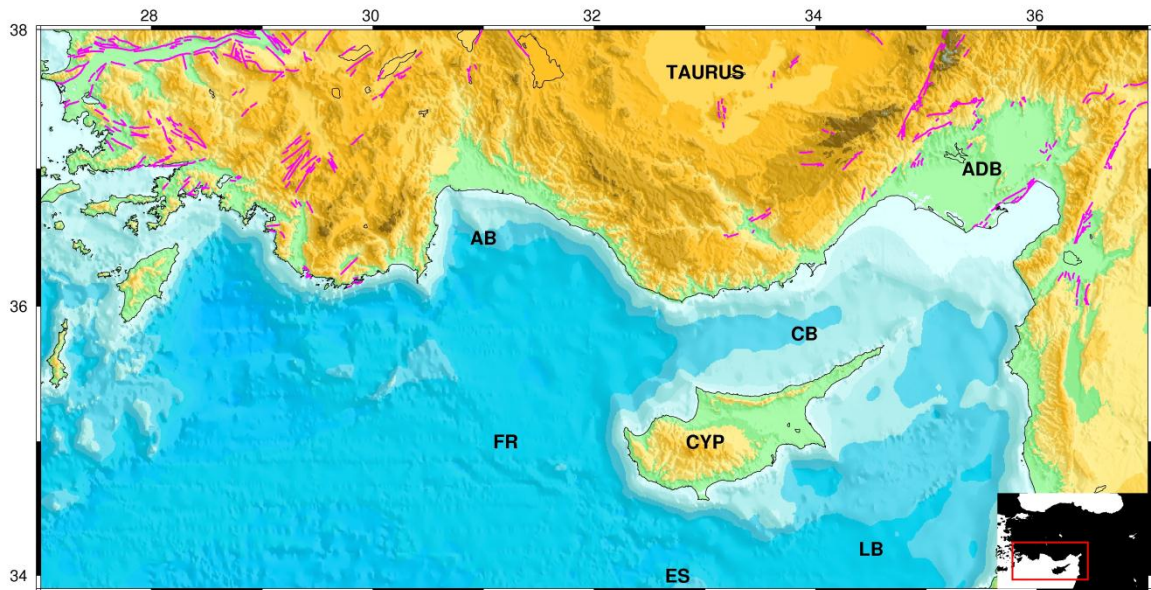


Figure 1.1. The map of the Eastern Mediterranean. AB: Antalya Basin; ADB: Adana Basin; CB: Cilicia Basin; LB: Levant Basin; FR: Florence Rise; ES: Eratosthenes Seamount; CYP: Cyprus. The red lines shows the major faults in the region (Robertson, 2000; Mutlu and Karabulut, 2011).

The Eastern Mediterranean crust has been studied extensively, nevertheless the nature of the crust, whether it is highly attenuated continental or oceanic, is still debated (Makris *et al.*, 1983; Ben-Avraham *et al.*, 2002; Dercourt *et al.*, 1986, Ginzburg and Ben-Avraham, 1987). Use of various active and passive source techniques (e.g. seismic refraction, reflection method and local earthquake tomography) provide essential information about the deeper parts of the Earth. They offer a number of advantages as an initial point for the construction of the crustal velocity structures. The most important disadvantage of active source experiment is the poor depth sampling. On the contrary, the main advantage of uncontrolled source technique is that it provides better coverage in depth to determine or provide constraints on the structure of the crust.

According to local tomographic study by Koulakov and Sobolev (2006), there is a high velocity oceanic crust under Levant basin while low velocity continental crust is found under Eratosthenes Seamount (Figure 1.1). However, lack of data coverage and poor azimuthal distribution of the stations gave rise to unreliable results about depth determination of the events. Biryol *et al.* (2011) performed teleseismic P wave

tomography. The aim of the study was to image the subducting African lithosphere along both the Aegean trench and particularly the Cyprean trench. Station coverage is sparse at this region in their study. The fast anomalies located to the north of the Cyprean trench are observed. While the Cyprus slab is subvertical at depths shallower than 200 km, there is a change in slab angle at a depth of 200-400 km. There is a gap of knowledge in this part of the Mediterranean, concerning the reliability of the data-sets, which we put together with adequate analysis.

Seismic refraction experiment conducted by Makris *et al.* (1983) suggested continental crust under Cyprus. Moreover, the velocity structure of the crust between Cyprus and Israel was obtained. Due to the lack of the ocean bottom seismometer on top of the Eratosthenes Seamount, the nature of the crust under the Eratosthenes Seamount was not known. The results showed continental crust under Cyprus is thinning southwards and extending to Eratosthenes Seamount. Ben-Avraham *et al.* (2002) suggested the presence of oceanic crust under portions of the Levant Basin and continental crust under the Eratosthenes Seamount. Furthermore, 10-14 km thick sediments are located in the Levant basin. Since the data were obtained at a water depth of about 1800 m, presence of the thick sedimentary sequence makes it difficult to obtain information in that area. Seismic refraction method performed by Netzeband *et al.* (2006) also showed thinned continental crust under the Levantine Basin. However, resolution of the results is insufficient to discriminate the type of crust.

Seismic velocity models play an important role in seismology as the starting point for various studies. They can be employed for improved location of earthquakes. Furthermore, they can be used as an initial model for seismic tomography studies. The tomographic results depend on the initial reference models and hypocentral locations. Most of the velocity models are obtained by first creating simple smooth 1-D models, which are iteratively updated to reach a minimum model.

The aim of this study is to construct 1D local crustal structures in the Antalya Bay, Adana Basin, Cyprus, Fethiye and Konya region. Seismic data are compiled from more than 250 stations operated by Kandilli Observatory and Earthquake Research Institute (KOERI), TUBITAK-MAM, AFAD and other temporary projects where the events are

recorded between 2005-2011. More than 2000 earthquakes are selected for the inversion process in this study.

The obtained Moho depth agrees with most of the other geophysical studies performed in the same area. Koulakov and Sobolev (2006) obtained 33 km Moho depth beneath Cyprus while Makris *et al.* (1983) computed Moho depth as 35 km. The Moho depth value obtained in our study is about 32 km. Moho depth changes from 30 km to 35 km beneath the Eastern Mediterranean (Tesauro *et al.*, 2007). Grad *et al.* (2009) obtained Moho depth that is varying from 30 km to 35 km beneath southern coast of Turkey and Cyprus. Furthermore, Moho depth is between 30-35 in the global crustal model, Crust 2.0 (Bassin *et al.*, 2000).

In this respect, I will pursue the following outline: Section 1 presents the geology and tectonic settings of southern Turkey as well as a brief discussion of the previous studies carried out in the study area. The methodology of velocity inversion for obtaining the minimum 1D model is summarized in the Section 2. Section 3 covers data processing conducted in this work. Inversion results and their analyses are given in Section 4. Section 5 presents the discussions of the study. The conclusions are presented in Section 6.

1.1. Geology and Tectonic Settings

The Eastern Mediterranean is a remnant of the Neo-Tethys ocean. Neo-Tethys has been formed by rifting phases along the northeastern margin of the Afro-Arabian Plate (Garfunkel and Derin 1985; Ben-Avraham and Ginzburg 1990; Garfunkel, 1998). The formation of the Levant basin is thought to be closely related to the evolution of the Neo-Tethys Ocean (Garfunkel, 1998). During the sea-floor spreading of the Atlantic Ocean, Neo-Tethys ocean is forced to close in the Late Triassic–Early Jurassic time with the commencement of the long-term subduction and accretion processes. This shaped the overall evolution of the Eastern Mediterranean (Dewey *et al.*, 1989; Garfunkel, 1998). When the last pieces of the oceanic lithosphere are consumed in the eastern Anatolia accretionary complex in the early Miocene, collision of the African and Eurasian Plates began. This collision plays a significant role in the tectonic evolution of the Eastern Mediterranean. Due to the collision of lithospheric plates, continental subduction

(Robertson *et al.*, 1998), strike-slip faulting and tectonic escape (McKenzie, 1972; Tapponnier *et al.*, 1982; Şengör *et al.*, 1985) crustal thickening (Şengör and Kidd, 1979), topographic build-up (Dewey *et al.*, 1986) and lithospheric-scale extension (Dewey, 1988) take place. To the west, subduction of the African lithosphere is still ongoing under the Hellenic trench (Şengör *et al.*, 2008, Dewey *et al.*, 1989).

The study area is situated on the plate boundary between the Anatolian microplate and the African Plate, and extending to the triple junction between the Anatolian, African and the Arabian Plates. Therefore, its kinematics is linked to these domains. Central Anatolia moves counterclockwise with 20-25 mm per year (Reilinger *et al.*, 2006). GPS measurements show that Anatolian velocities increase with respect to Eurasia from east to west in an anti-clockwise fashion (McClusky *et al.*, 2000; Reilinger *et al.*, 2006). The motion of Arabian Plate is NNE with constant velocity of 25 mm per year since 40 Ma. The relative motion between Arabian Plate and Anatolia is compatible with EAF as 9 ± 1 mm per year slip rate (McClusky *et al.*, 2000). Therefore, in our study, along the western part of Cyprus Arc, the convergence rate increases northwestwards and is 9–14 mm per year. Along the southern section of the western side of the arc, the convergence rate is about 7–8 mm per year (Wdowinski *et al.*, 2006). Africa–Arabia GPS Euler vector shows 5.8 ± 1 mm per year left-lateral slip on the southern Dead Sea fault (McClusky *et al.*, 2003).

Antalya Bay is a key region located on the western flank of the Cyprus Subduction Zone (CSZ), close to the junction between the Hellenic and Cyprus Arcs. It separates the African Plate in the south from the Anatolian Plate in the north in the eastern Mediterranean (McKenzie, 1970, Smith, 1971, Ryan *et al.*, 1971, McKenzie, 1972, Dewey *et al.*, 1973, Nur and Ben-Avraham, 1978, Garfunkel, 1998, Vidal *et al.*, 2000). Antalya Basin is dominated by thick sedimentary succession reaching at least 1500 m (Woodside *et al.*, 2002, Ergün *et al.*, 2005). The Konya region in central Anatolia is covered by Pliocene–Late Pleistocene sediments and volcanic units (Karakaya *et al.*, 2004). The Adana–Cilicia Basin takes place between the early Cenozoic Tauride belt and late Cenozoic Cyprus lineament (Özel *et al.* 2007). Evolution of the Adana Basin contains an early period of peripheral foreland basin development completed in the late Miocene/early Pliocene by a transtensional regime created during the westward tectonic escape of

Anatolia and following inception of the Kahramanmaras triple junction (Şengör *et al.*, 1985). Crustal fragments can be seen as ophiolite sequences in Cyprus (Moores and Vine, 1971) (Figure 1.2). In fethiye region, Finike Basin contains thick Pliocene-Quaternary successions (Aksu *et al.*, 2009).

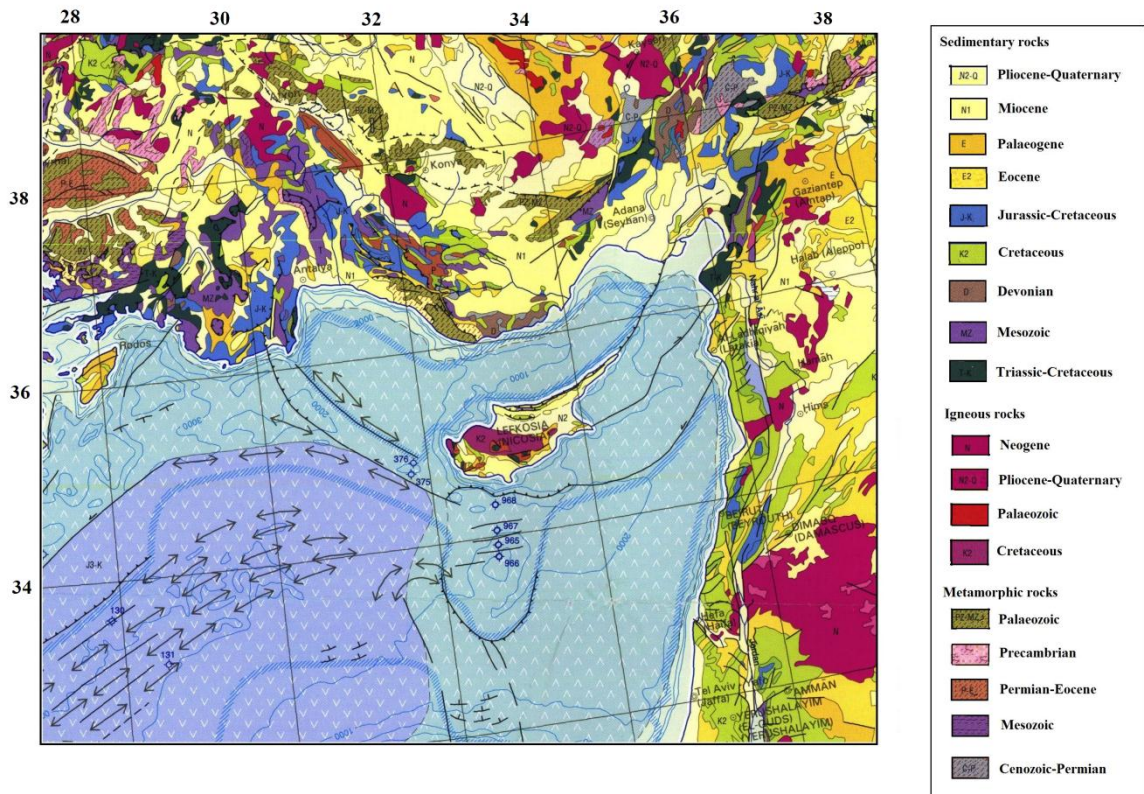


Figure 1.2. Geological map of the Eastern Mediterranean (Asch *et al.*, 2004).

1.2. Seismotectonics of the study area

In the study area, earthquakes cluster around Adana, Cyprus, Fethiye, Antalya and Konya region. There are also earthquake clusters in the north of Tuz Lake, northwest and west of Antalya region. Adana region is dominated by strike slip and normal events while majority of focal mechanisms are oblique in Fethiye region. The north of the Tuz Lake comprises of strike slip events. In Konya region, normal events are observed. West of Antalya region also consists of normal events (Figure 1.3).

The Cyprian Arc is an active plate boundary located between the African Plate in the south and the Anatolian Plate in the North (McKenzie, 1972; Garfunkel, 1998). Arc geometry plays a significant role in tectonic along the arc. Eastern part of the arc is almost parallel while western part is perpendicular to the direction of relative plate motion. Wdowinski *et al.* (2006) investigated the Cyprian subduction zone by dividing it in four segments, which is categorized in terms of style of faulting.

In the northwestern part of the arc is characterized by normal and reverse events. Deep earthquakes (>40 km), which are shown in red, are nucleated beneath Antalya basin. They reveal that subduction occurs at the western flank of the arc. However, shallow events (<40 km), shown in purple, take place at the southwestern Cyprus (Figure 1.3). It is dominated by strike slip and thrust earthquakes. Large earthquakes are observed at this part. The 1996 Paphos Earthquake ($M_w=6.8$) which is defined as the largest earthquake occurred at southwestern Cyprus (Arvidsson *et al.*, 1998; Pilidou *et al.*, 2004). Northeastern part of the arc consists of strike slip and normal events. The 1998 Adana Earthquake ($M_w=6.2$) took place at this segment (Aktar *et al.*, 2000). Thrust events take place at southeastern Cyprus (Wdowinski *et al.*, 2006). Though in CMT catalogue those events have not been relocated (see Figure 1.3 below for the recent compilation of FMS). These thrust events can be interpreted as incipient collision occurring at southeastern Cyprus (Wdowinski *et al.*, 2006). The collision between Cyprus and the Eratosthenes Seamount has been identified by Robertson *et al.* (1998) and findings of Wdowinski *et al.* (2006) show that an eastward continuation of this collision may be underway.

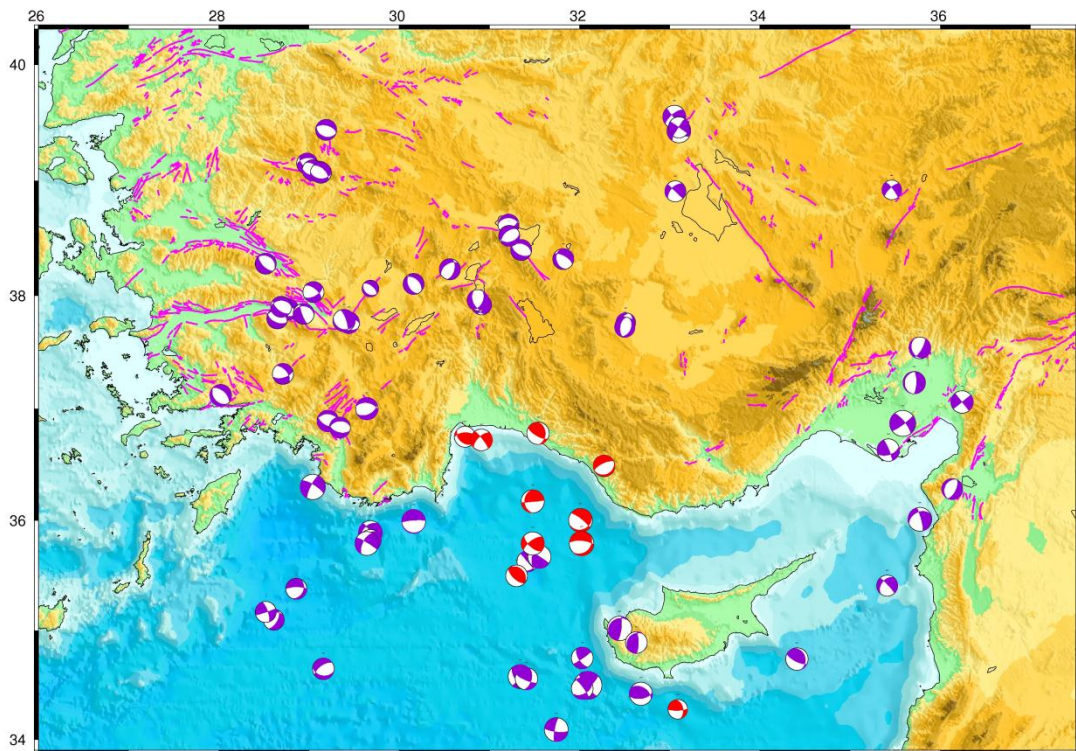


Figure 1.3. Focal mechanism solutions (taken from Harvard CMT Catalog). Deep earthquakes (>40 km) are shown in red while shallow events are shown in purple.

1.3. Previous Studies

Various studies have been made to gain insight about the crustal structure beneath the Eastern Mediterranean. Local tomographic study by Koulakov and Sobolev (2006) revealed the velocity model of the crust and uppermost mantle in the Eastern Mediterranean. They employed seismic data between 1964–2001, which were recorded at about 250 seismic stations. More than 80,000 P and S arrivals were used to determine detailed structure of the crust and the uppermost mantle. They observed that the crustal thickness varies from 33 km in Cyprus to 27 km under Eratosthenes Seamount. Low velocities were observed under the Cyprus which shows continental crust. However, higher velocities were obtained under the Levant Basin which indicates oceanic crust. In the Levant basin, the crustal thickness is about 19 km, while in the continental parts the Moho depth changes between 27 and 37 km.

Piromallo and Morelli (2003) performed seismic travel time tomography for the Mediterranean area. The aim of their study was to determine the upper mantle P wave velocity structure. They used selected 52,000 events between the years 1964-1995. They observed a small magnitude fast P velocity perturbation near the Antalya basin, which can be explained with the termination of the Cyprean trench. Spakman (1991) used seismic tomography in order to determine P velocity structure of upper mantle in the Mediterranean area. He obtained positive anomalies underneath the Antalya Basin where the Cyprus Arc intersects coast of Turkey. A smaller part of the Eastern Mediterranean, where Cyprean and Aegean trenches are located, was studied by Biryol *et al.* (2011). They used 201 seismic stations and 409 teleseismic events between 1999-2009. According to Biryol *et al.* (2011), a fast anomaly which may be related to the subducted portion of the African lithosphere was observed in the north of the Cyprean trench. There is a subvertical slab at depth shallower than 200 km. Angle of the slab changes significantly at depths between 200 and 400 km. Mutlu and Karabulut (2011) presented an analysis of Pn traveltimes to determine lateral variations of velocity, anisotropy of uppermost mantle and crustal thickness beneath Turkey and adjacent regions. They observed significant crustal thickening beneath the Antalya bay with larger Pn velocities associated with the subducting plate.

Boschi *et al.* (2004) performed surface wave tomography of the Mediterranean basin. Low velocity anomalies were obtained under Levant Basin, southeastern Mediterranean. However, higher velocities were observed under the Levant Basin by Koulakov and Sobolev (2006). Kustowski *et al.* (2008) studied the shear wave velocity structure in the upper mantle. The model reveals fast velocities beneath the Mediterranean basin at 350 and 500 km, which are related to tectonic convergence. Salaün *et al.* (2011) presented new constraints on the upper-mantle structure from western Greece to central Anatolia using seismic data of permanent broad-band networks recently installed in Greece and Turkey and from a two-year temporary array (SIMBAAD experiment) by performing Rayleigh wave tomography. They showed the presence of the slab beneath the Antalya bay to a depth of 300 km and a possible slab tear between the Antalya bay and Cyprus.

Series of seismic refraction experiments were carried out in the eastern Mediterranean. Makris *et al.* (1983) showed between Eratosthenes Seamount and the Israel

crust is composed of high velocity material and is about 8 km thick. It may indicate an oceanic crust while the island of Cyprus has 6 km/s continental crust. Ben-Avraham *et al.* (2002) studied the Levant basin with the seismic refraction method, in combination with reinterpretation of Makris *et al.*'s (1983) refraction line. Seismic data were recorded at land stations and ocean bottom seismometers. The results indicated that crust is oceanic under the Levant Basin while it is continental under the Eratosthenes Seamount. This is evidenced the 6.0 km/s layer and the presence of a higher velocity (6.7 km/s) crust underneath the Eratosthenes Seamount. They also demonstrated there is about 10-14 km sedimentary layer in the Levant Basin. Netzeband *et al.* (2006) also suggested thinned continental crust under the Levantine Basin. However, velocity models and structure of the crust along profiles do not present typical features of oceanic or continental crust.

Gravity study by Khair and Tsokas (1999) revealed Moho depth ranges from about 20 km to about 28 km below sea level in the Eastern Mediterranean. Ergün *et al.* (2005) also suggested low gravity anomalies indicate the boundary between the African and Aegean/Anatolian plates at basement level. Thick sediments which may have filled the former trench at the subduction zone lead to low anomalies in the region.

2. METHOD

One-dimensional (1D) velocity models are widely used to locate earthquakes at seismological observatories and in regions where three-dimensional (3D) velocity models are not available due to the lack of high quality data. The 1D models with the corresponding station corrections also provides a framework to compute initial hypocenter locations and seismic velocities for local earthquake tomography. However, a simple 1D velocity structure with station delays may not always be appropriate for the complex tectonic regions with significant three-dimensional (3D) variations in seismic velocities. A better choice is to compute several local minimum 1D models for tectonically complex regions. In this study, we compare the earthquake locations with one regional minimum 1D model and local minimum 1D models for the selected subregions of the Southern Turkey, which exhibits Moho topography.

The minimum 1D model has been proposed as the best velocity model to derive reliable initial hypocenter locations and seismic velocities for local earthquake tomography (Kissling *et al.*, 1994). The computation of a minimum 1D model solves a coupled hypocenter-velocity problem, and thus it also provides suitable velocity models for routine earthquake location. The forward problem is solved by ray tracing from source to receiver (Kissling, 1988).

Travel time of a seismic body wave (T) from an earthquake i to a seismic station j is expressed by using ray theory as a path integral;

$$T_{ij} = \int_{\text{source}}^{\text{receiver}} u ds \quad (2.1)$$

where u refers to the slowness field (reciprocal of velocity) and ds is an element of path length.

The body wave arrival time (t_{ij}) can be written as;

$$t_{ij} = \tau_i + T_{ij} \quad (2.2)$$

where τ_i is origin time of the event. The coordinates of the source, origin times, ray paths, and the slowness field (the model parameters) are unknown. Equation 2.1 and 2.2 are used to calculate t_{ij}^{obs} .

$$t_{ij}^{\text{res}} = t_{ij}^{\text{obs}} - t_{ij}^{\text{cal}} \quad (2.3)$$

Travel time of a seismic wave through the distance between hypocenter and a station can also be defined as a nonlinear function of hypocentral parameters and velocity field.

$$t_{\text{obs}} = F(t_0, x_0, y_0, z_0, V(x, y, z)) \quad (2.4)$$

where t_0 is origin time, x_0, y_0, z_0 are latitude, longitude and depth, respectively. $V(x, y, z)$ represents velocity field.

The true hypocentral parameters and velocity field are not known while arrival times and station location are known. Equation can not be solved with only travel times and station location. Theoretical arrival times (t_{ij}^{calc}) can be determined with the help of a priori velocity model. The residual travel time (t_{ij}^{res}), which can be defined as the differences between the observed and the calculated travel time, can be written as functions of the differences between the estimated and the calculated hypocentral and velocity parameters (Kissling *et al.*, 1994).

$$t_{ij}^{\text{res}} = \sum_{k=1,4} \frac{\partial T_{ij}}{\partial h_k} \cdot \Delta h_k + \sum_{i=1,n} \frac{\partial T_{ij}}{\partial m_i} \cdot \Delta m_i + e \quad (2.5)$$

t represents vector of travel time residuals, h represents vector of hypocentral parameter adjustments, m is vector of model parameter adjustments and e is vector of travel time errors, containing errors in measuring the observed travel times, errors in the calculated travel times because of errors in station coordinates, application of the wrong velocity model and hypocentral coordinates, and errors created by the linear approximation.

Equation 2.5 may be written as;

$$t = A.d + e \quad (2.6)$$

where A is matrix of all partial derivatives and d is vector of hypocentral and model parameter adjustments (Kissling *et al.*, 1994).

$$A = \left[\begin{array}{ccc|ccc} \frac{\partial t_i}{\partial h_{1,j}} & 0 & 0 & \frac{\partial t_i}{\partial m_1} & \dots & \frac{\partial t_i}{\partial m_n} \\ 0 & \dots & 0 & \frac{\partial t_i}{\partial m_1} & \dots & \frac{\partial t_i}{\partial m_n} \\ 0 & 0 & \frac{\partial t_i}{\partial h_{n,dep,j}} & \frac{\partial t_i}{\partial m_1} & \dots & \frac{\partial t_i}{\partial m_n} \end{array} \right] \quad (2.7)$$

The first part of the matrix A represents partial derivatives of hypocentral parameters while the second part corresponds to model parameters.

Equation 2.6 can be written as;

$$t = A.d + e = Hh + Mm + e \quad (2.8)$$

where H is matrix of partial derivatives of travel time with regard to hypocentral parameters, M refers to matrix of partial derivatives of travel time concerning model parameters.

3. DATA PROCESSING

A minimum 1D model approximate a weighted average of the data and reflect the overall features of the structure investigated. The computation of a 1D model starts with the definition of three elements:

- 1- the region of application,
- 2- the layering of the a-priori 1D velocity model,
- 3- the quality selection of the local earthquake data-set and a station list (Kissling, 1995).

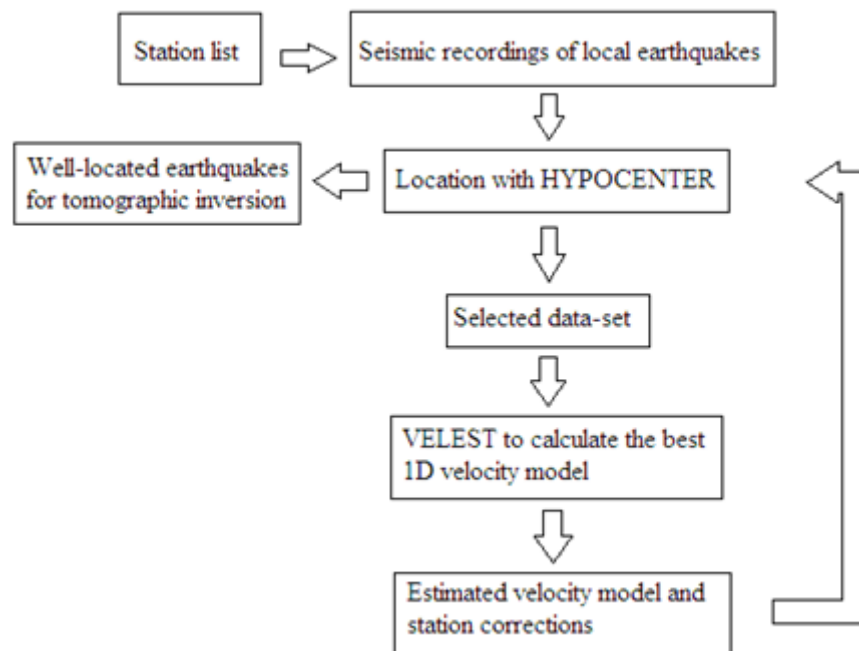


Figure 3.1. Diagram of the inversion procedure for the computation of the 1D Minimum velocity model.

Our study region is bordered by 26-37.5° E and 33.9-40.30° N as shown in the Figure 3.5. Within the region of interest, more than 10 000 earthquakes have been located for the time period between 2005–2011 (Figure 3.5), by using a-priori velocity model and the hypocenter program is a modified version of HYPOCENTER (Lienert *et al.*, 1986, Lienert, 1991, Lienert and Havskov, 1995).

More than 250 temporary and permanent seismic stations operated by several agencies and experiments are used (Figure 3.4). In this study, earthquakes can be grouped in several distinct clusters. We cluster the data according to their spatial proximity to each other because similar waveforms of the events enable us to pick precise arrival times. Therefore, clusters may lead to improved velocity structure determination. We also group larger areas, which include clusters, in order to locate with obtained velocity models. We try to distinguish tectonic structures which are close to each other.

A filtering of this data-base, with respect to their quality, has been carried out, as large uncertainties in hypocenter locations introduce instabilities during the inversion process. Well-located events were selected using the criteria of a minimal number of 3 P-phases, $\text{RMS} \leq 1$ s, hypocentral errors ≤ 25 km and a maximum gap of 270° . The maximum gap is an important parameter for selection that ensures that events are well localizable by the local network. The resulting data-set is comprised of more than 2000 earthquakes, with a total of 4500 events. Figure 3.7 illustrates the number of observations for each station.

The selected events are inverted by using the program VELEST (Kissling, 1995) to calculate the adjustments of P-wave velocities (layer depths are kept fixed) and station corrections. We assumed a V_p/V_s value equal to 1.73. The model damping parameters were chosen after optimizing the data misfit reduction and the parameter resolution. The inversion process was stopped when the earthquake locations, the station corrections and the velocity values did not vary significantly in subsequent iterations. After calculation of velocity models, we locate P-wave velocities (layer depths are kept fixed) and station corrections. The earthquakes are relocated using the local velocity models and station corrections. However, tomographic inversion is not applied to the well-located earthquakes in our study. An outline of the inversion procedure for the computation of the 1D Minimum velocity model is presented in Figure 3.1.

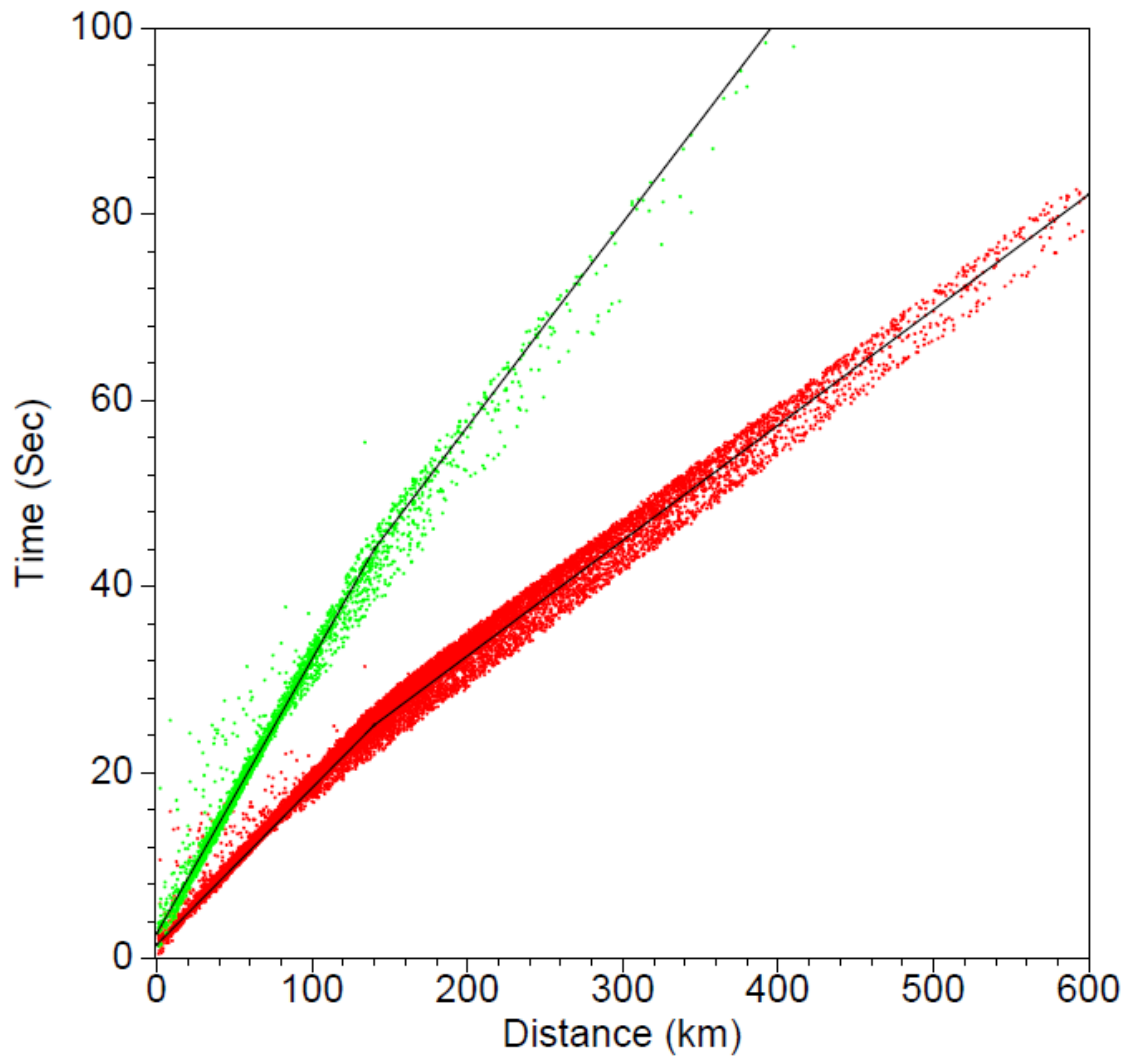


Figure 3.2. Travel time arrivals of P (red) and S (green) phases. Black lines show the least squares fits to the travel times.

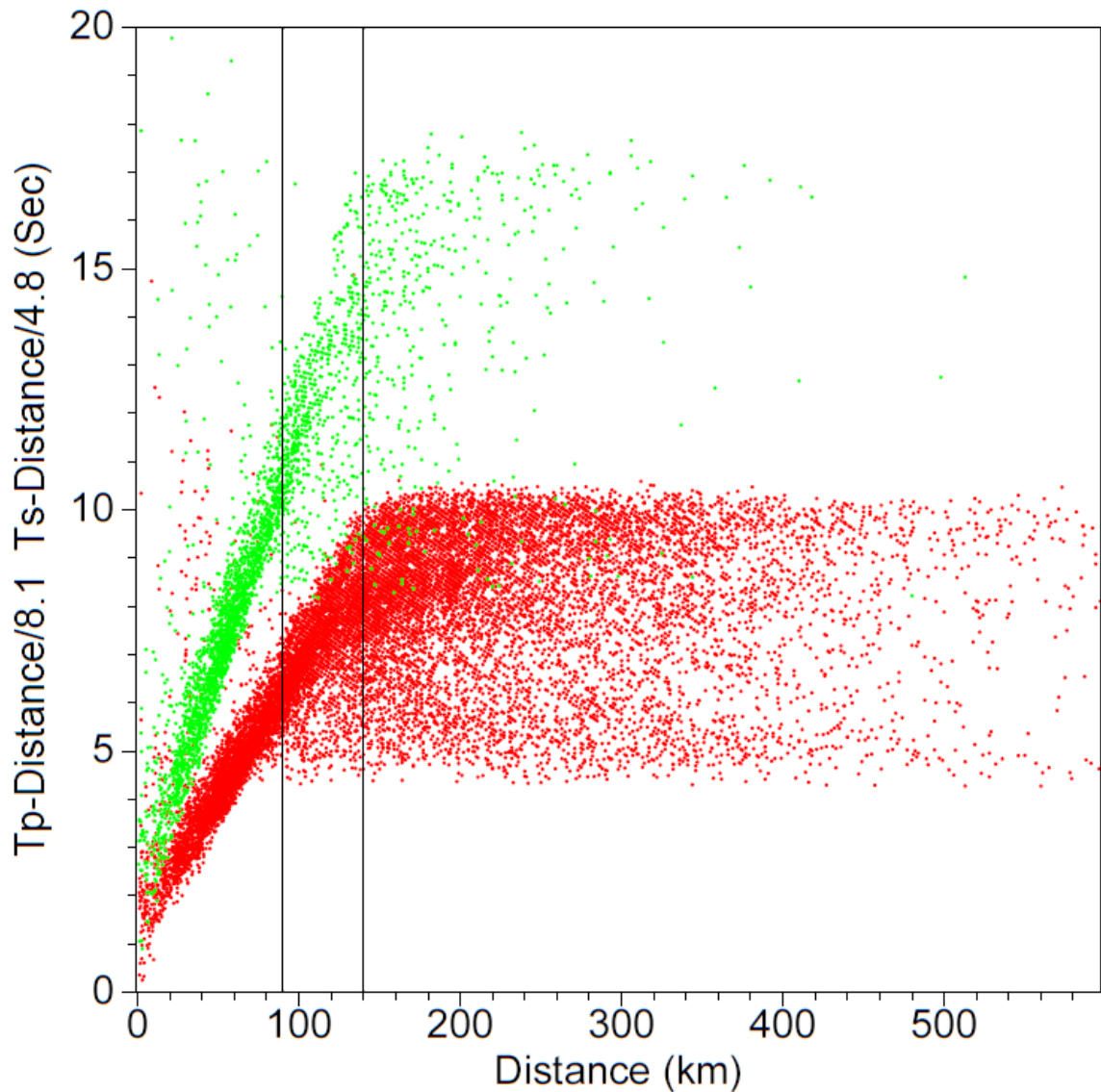


Figure 3.3. Reduced travel time arrivals of P (red) and S (green) phases. Black lines show the range for critical distances.

Figure 3.2 shows that P and S travel time of the earthquakes versus distance curve. Velocities of subsurface layers can be calculated directly from the reciprocal slopes of the straight lines corresponding to the direct and refracted rays. When the velocities are determined, it is possible to compute the Moho depth by using the crossover distance, which can be read directly from the travel time–distance plot. The cross over distance is the distance at which the first arrival times are direct signals. It marks the point when the refracted wave overtakes and arrives before the direct wave. Cross over distance is about

140 km (Figure 3.3). Moho depth is around 31 km. The initial models are based on perturbations of this average crustal thickness.

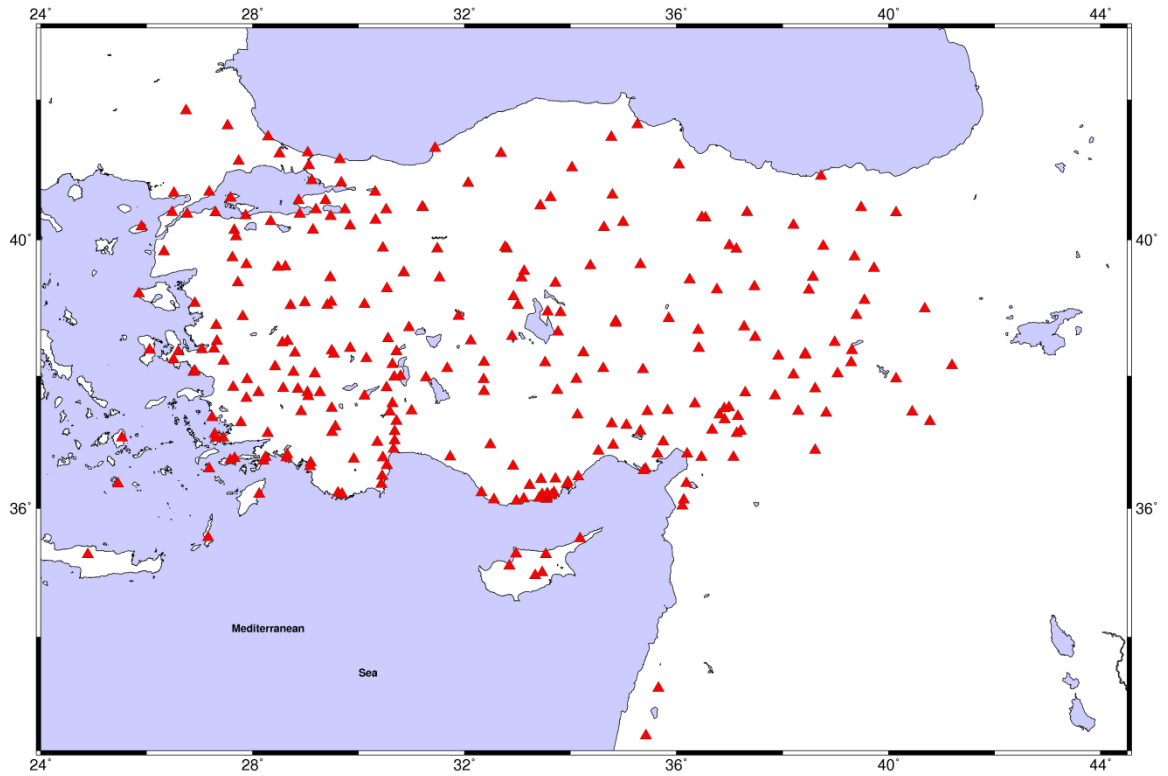


Figure 3.4. Distribution of stations, which are used to locate earthquakes in the study region.

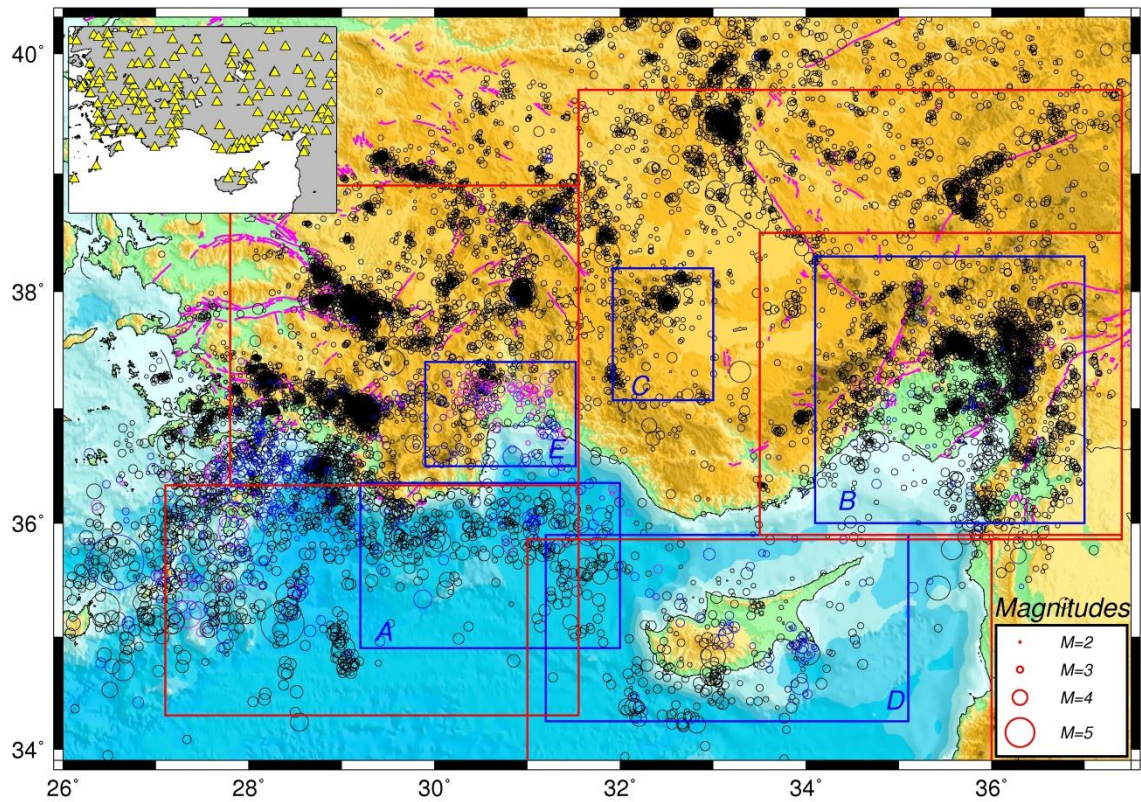


Figure 3.5. Seismicity of southern Turkey between 2005-2011. Blue frames indicate the earthquake clusters, where the total number of events is more than 4500, among which we selected over 2000 events with the highest data quality is chosen to construct 1-D velocity model. Red frames indicate representative regions for the 1-D velocity models, where we relocate each event with the corresponding blue frame. A, B, C, D and E refers to Fethiye, Adana, Konya, Kıbrıs and Antalya region, respectively.

Most of the events which are listed in the earthquake catalog contain location errors are about 2 km, 2 km and 4 km for latitude, longitude and depth, respectively. Majority of the earthquakes have 100 degrees azimuthal gap. The depth distribution demonstrates that most of the events are shallower than 25 km. Most events are recorded by 10 stations (Figure 3.6).

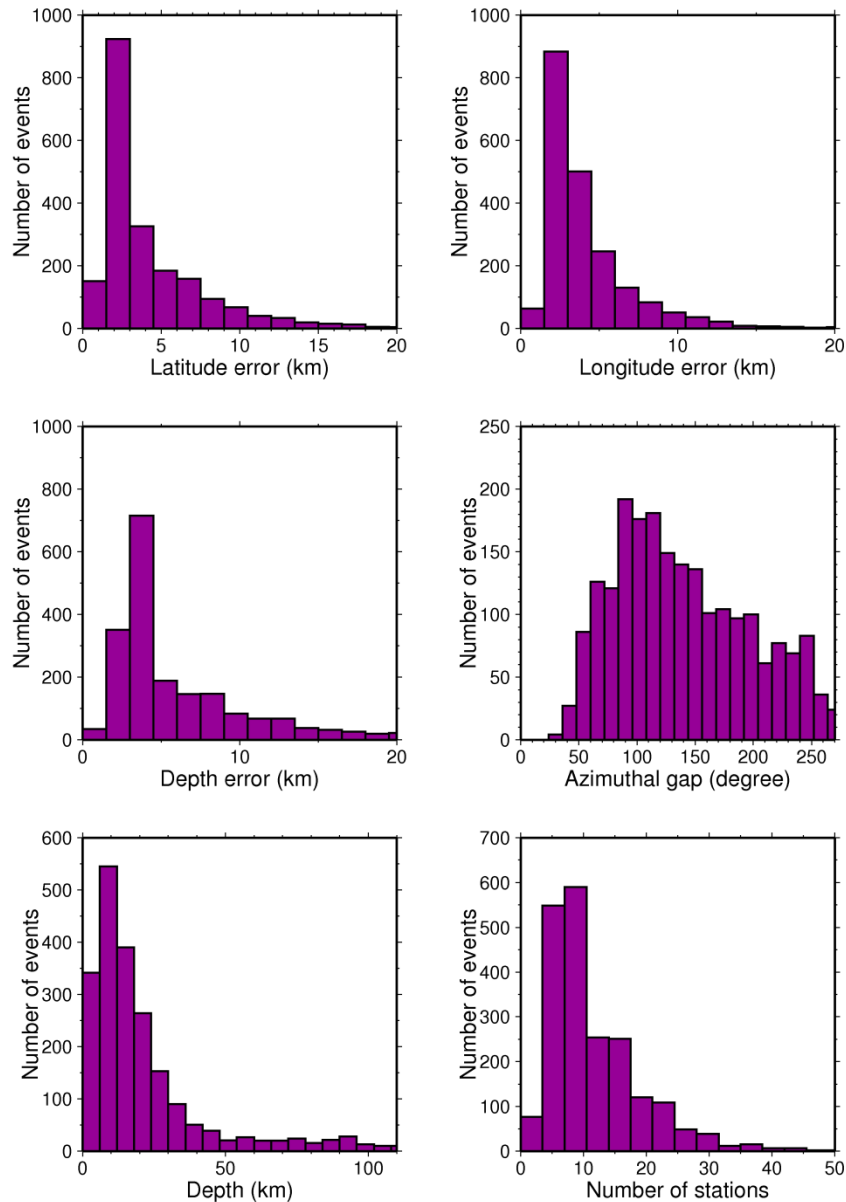


Figure 3.6. The statistics of the initial catalog with the locations computed using the 1D velocity model and no station correction.

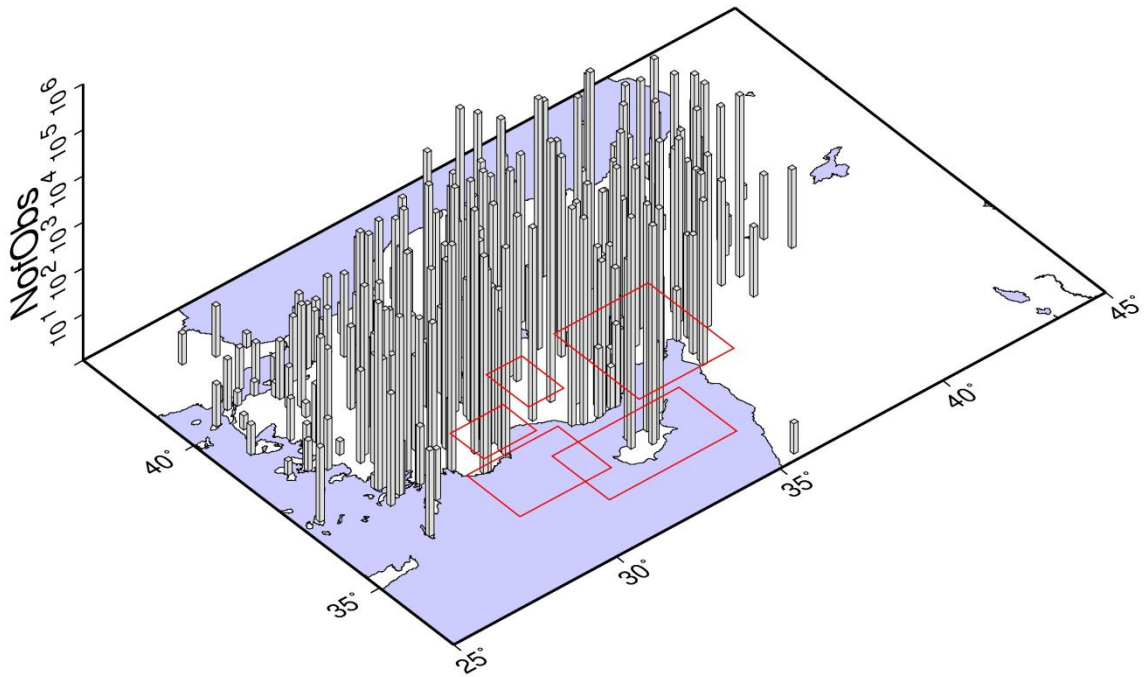


Figure 3.7. The number of observations for each station.

It can be noticed that stations around and within chosen areas have higher number of observations than other stations (Figure 3.7).

4. RESULTS

For five earthquake clusters, P and S wave first arrival times are inverted to obtain the 1D velocity model. For each cluster, 100 final velocity models for 100 different initial velocity models are obtained. The 100 initial models are computed by random perturbations of an initial velocity model. The earthquakes are relocated by using the best velocity model and station corrections. Station corrections are an important part of the 1D velocity model. They include the effects of surface geology. Negative station corrections define high velocities while positive ones indicate presence of low velocities with respect to the crust beneath the reference station. If the correction is negative, it means that the observed velocity is smaller than the calculated; in other words calculated velocities are slower than that of the model. Below I analyze each cluster in the light of velocity model and station corrections.

4.1. Region A: Fethiye

4.1.1. Hypocentral locations

Fethiye region is defined as A in Figure 3.5. The selected data-set is composed of 400 events out of 535 events. Relocated earthquakes display a decrease of RMS value. The total RMS value of all events decreased from 0.492 to 0.339. With the new velocity model, the quality of relocated events significantly improves due to the significant reduction of travel time residuals. The reference station is AKAS (Figure 4.1-inset). AKAS is near the center of the events.

By using the minimum 1D velocity model, a small shift of the most part of locations toward reference station is observed (Figure 4.1). Most of events in region A occur in the lower crust (hypocentral depth less than 30 km). In other words, majority of the events are shallower earthquakes. A small number of events takes place deeper in the crust and also below the Moho. Deep earthquakes are observed near Antalya Bay, which provide useful information about the seismotectonics of the region A.

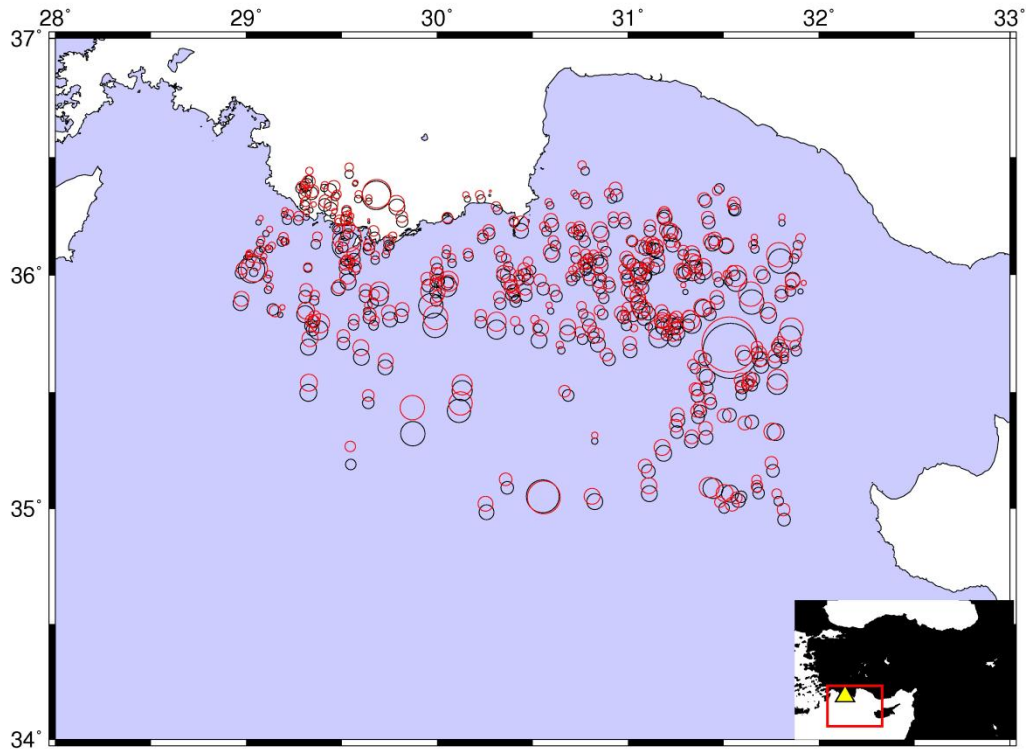


Figure 4.1. Relocated earthquakes for sub-region A. Red circles indicate the earthquakes with the 1D local velocity model obtained from VELEST. Black circles show the earthquakes with initial velocity model. Yellow triangle shows reference station AKAS.

4.1.2. Station corrections

The station corrections are given as relative value with respect to the reference station of AKAS (Figure 4.2).

Positive corrections of stations are observed in region B, suggesting the presence of lower velocities in the crust. It may be related to the presence of a thicker sedimentary Adana basin. In region C, which corresponds to Konya region, the values change between 0 and 0.7 s, which indicate lower velocities. Lower velocities may be indication of Pliocene–Late Pleistocene sediments and volcanics in Konya region. Station corrections range between -0.1 and -1 s in region D. As a result, higher velocities present in Cyprus. In region E, which is defined as Antalya region, generally positive station corrections are obtained. Lower velocities may be related to the sediments.

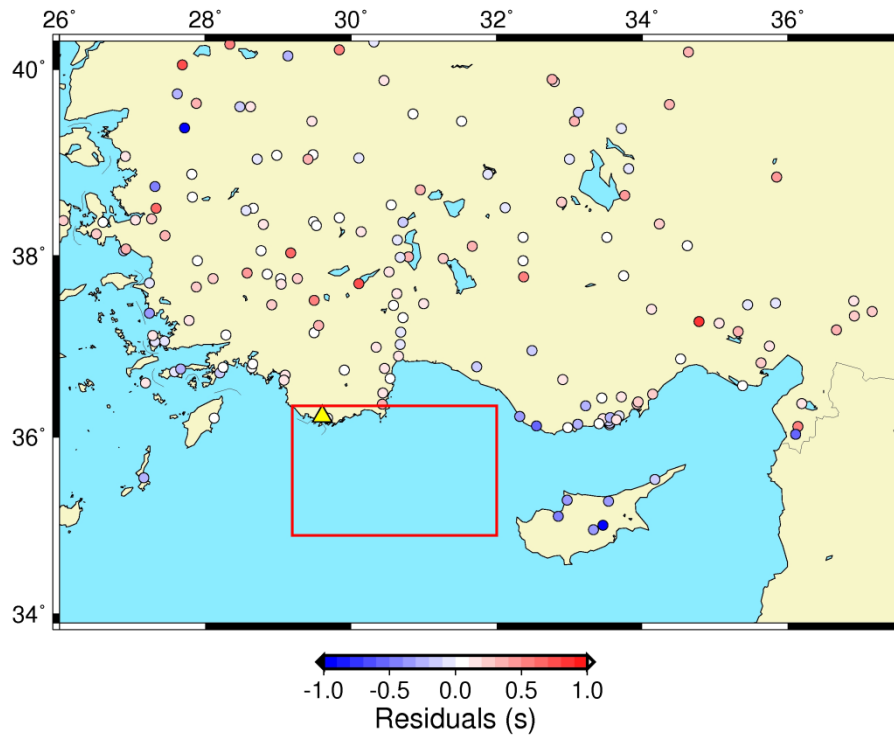


Figure 4.2. Station corrections of the earthquake cluster in sub-region A. Triangle shows the reference station for this cluster.

4.1.3. Velocity model

We observed an increase of velocity with depth (Figure 4.4). Value about 6 km/s is found for the upper crust. When passing through the Conrad discontinuity, velocity of P wave increases from approximately 5.8 km/s to 6.2 km/s while S wave velocity increases to 3.5 km/s. For the lower crust, around 6.4 km/s is calculated. Seismic velocities for these layers are well constrained, which is inferred from the depth distribution of the earthquakes.

At a depth of 32 km, P wave velocity is about 7.5 km/s while S wave velocity is 4.2 km/s. The jump from 6.8 to 7.5 km/s clearly shows the Moho discontinuity.

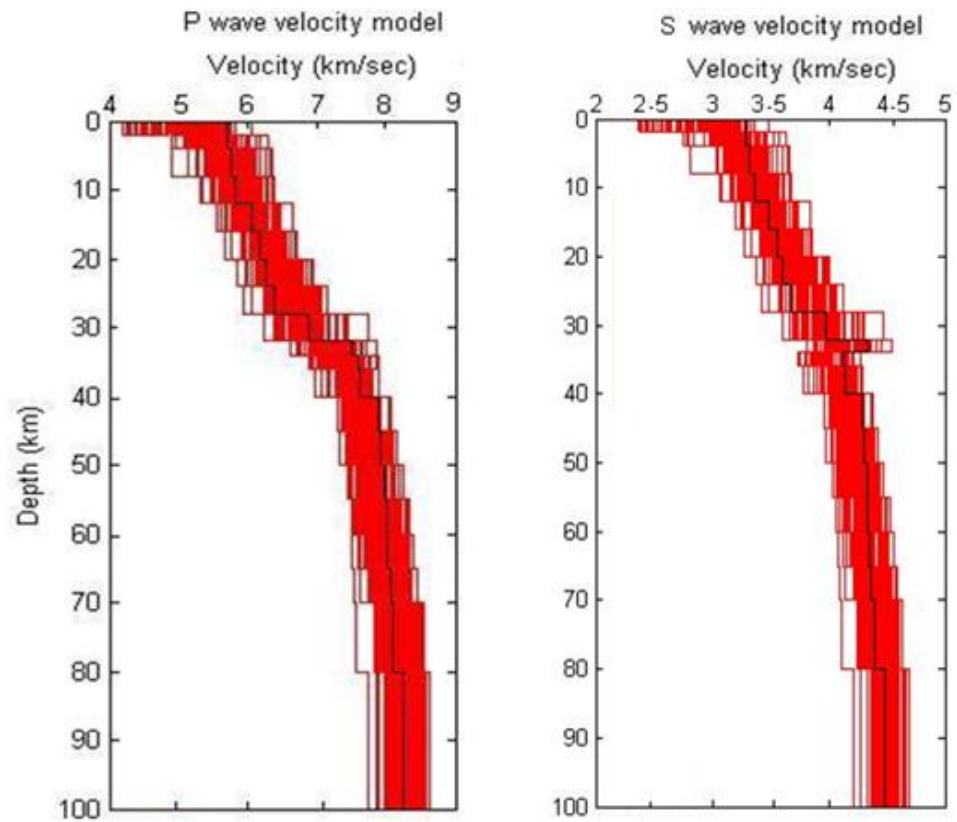


Figure 4.3. P and S wave initial velocity models of the earthquake cluster in sub-region A. Red lines show 100 randomly computed velocity models from an initial model constructed for the region A. The black one shows the initial velocity model for the best final velocity model in Figure 4.4.

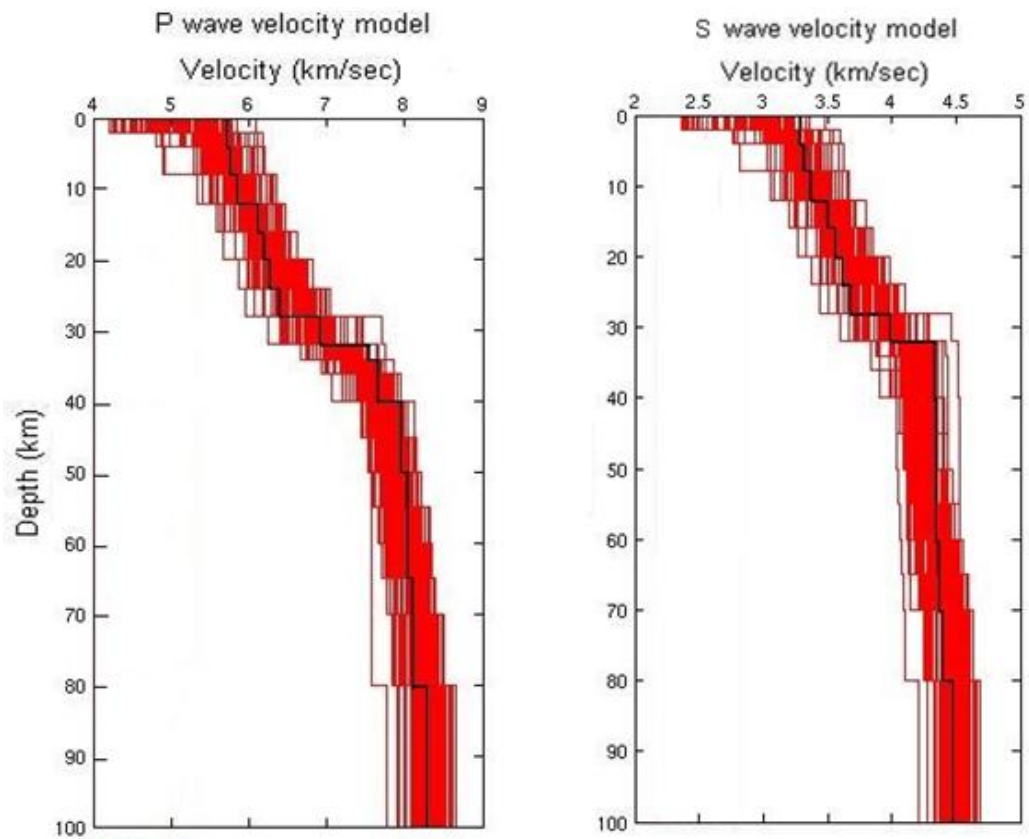


Figure 4.4. P and S wave velocity model of the earthquake cluster in sub-region A. Red lines show 100 final velocity models from the initial model in Figure 4.3. The thick black line shows the best velocity model.

4.1.4. Statistical properties

Average location errors are 4 km, 3 km and 5 km for latitude, longitude and depth, respectively. Average azimuthal gap is 200 degrees. The depth distribution demonstrates that most of the events in region A are shallower than 50 km. Most of the events are recorded by more than five stations.

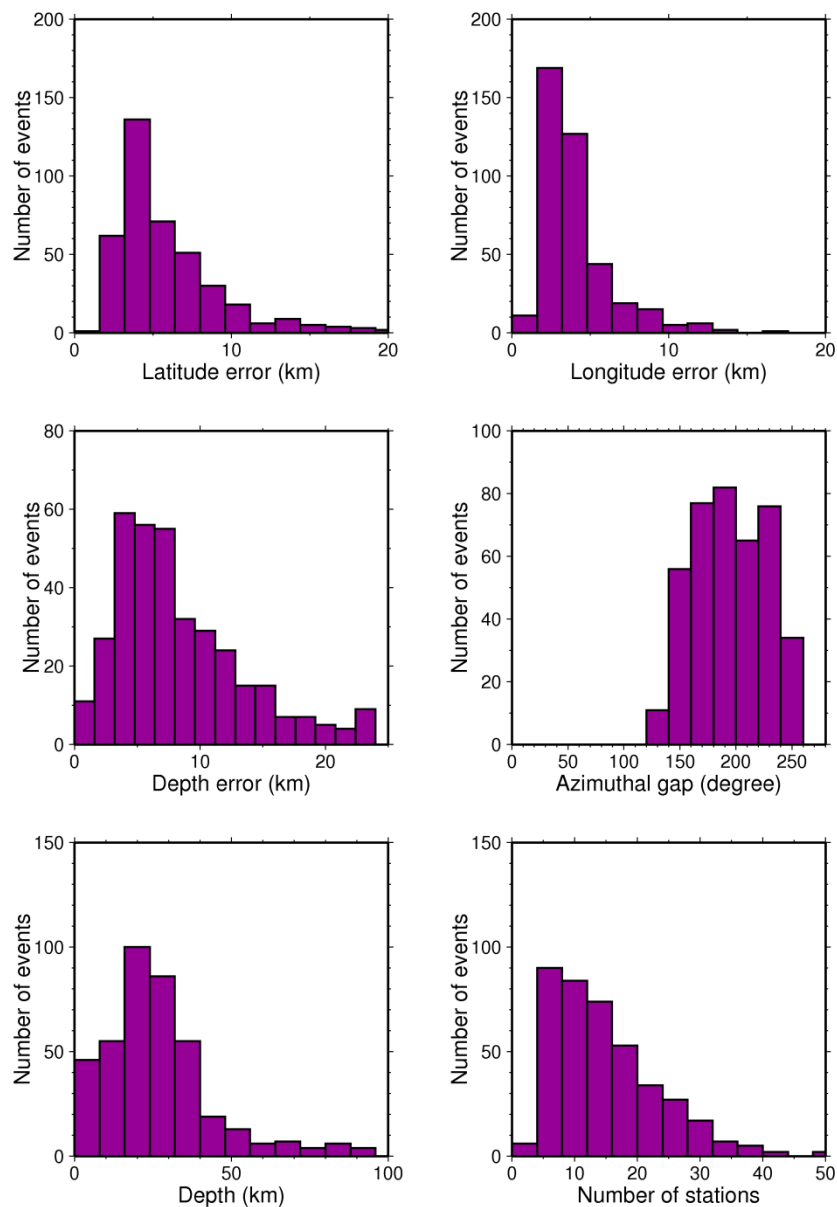


Figure 4.5. Statistics of the catalog for the earthquake cluster in sub-region A.

4.2. Region B: Adana

4.2.1. Hypocentral locations

Adana region is defined as B in Figure 3.5. A selection of 690 seismic events was inverted. YURE is chosen as reference station (Figure 4.6). Relocated earthquakes present a significant decrease of RMS values. Satisfactory reduction in RMS value is from 1.41 to 0.23. We are satisfied with the relocations because of the reduction of rms and small values of gap. The smaller these numbers, the more reliable is the hypocenter of the earthquake.

We observed a shift of most of earthquake locations to the reference station. Most of the earthquakes in region B occur in the upper and middle crust (hypocentral depth less than 20 km). There are a small number of events in the lower crust.

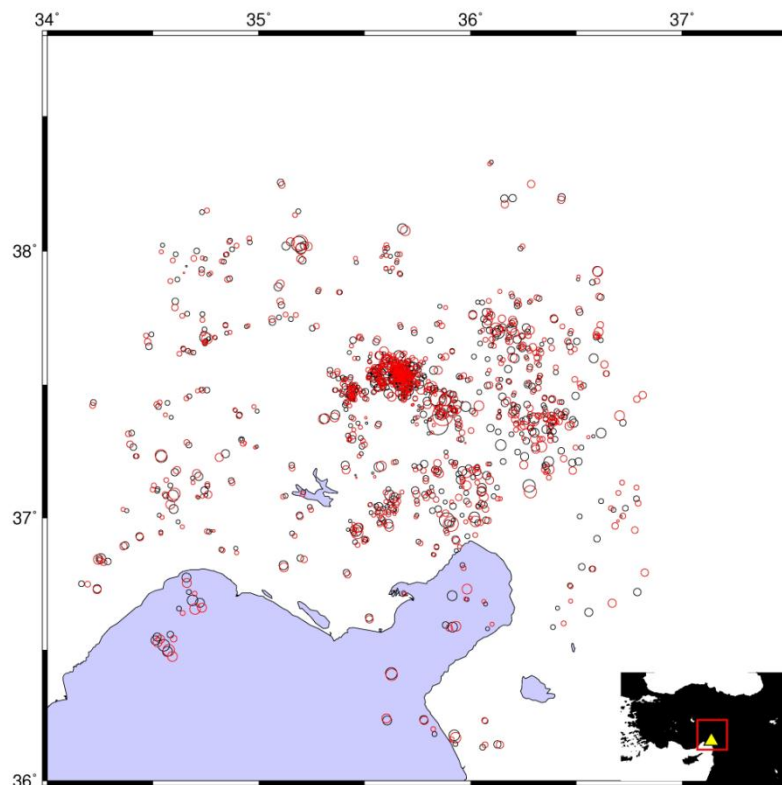


Figure 4.6. Relocated earthquakes for sub-region B. Red circles indicate the earthquakes with the 1D local velocity model obtained from VELEST. Black circles show the earthquakes with initial velocity model. Yellow triangle shows reference station YURE.

4.2.2. Station corrections

The station corrections are obtained as relative value with respect to the reference station of YURE (Figure 4.7-inset).

In contrast to station correction results of cluster A, for all regions, station correction values range between 0 and -0.7 s. Only in Cyprus region, almost the same values are obtained.

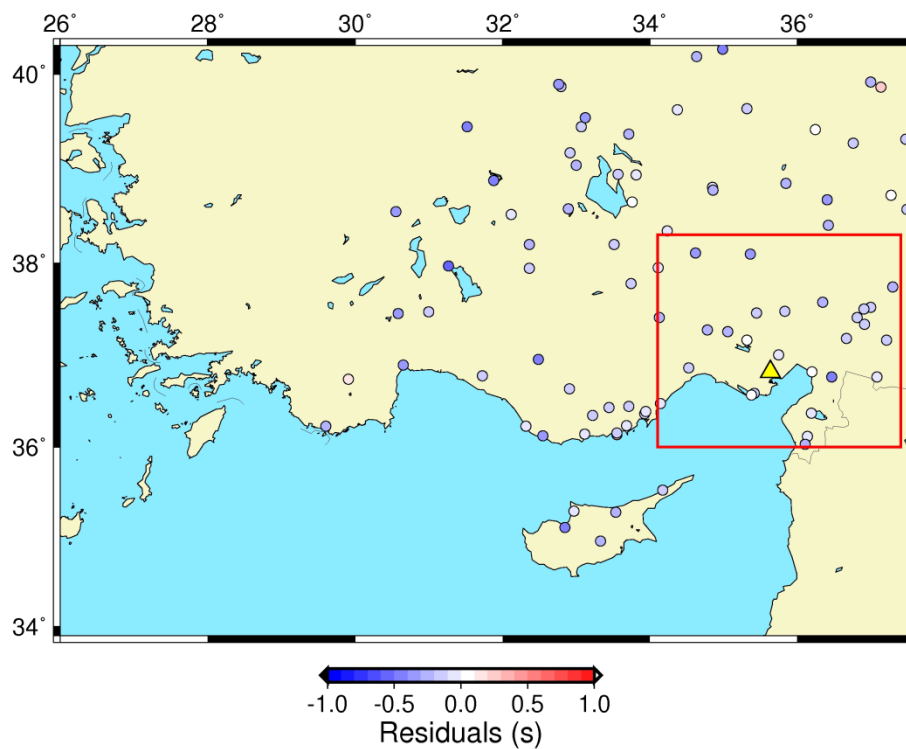


Figure 4.7. Station corrections of the earthquake cluster in sub-region B. Triangle shows the reference station for this cluster.

4.2.3. Velocity model

Low P and S velocities are obtained in shallower parts (~ 5 km) (Figure 4.9). At about 12 km, 6 km/s is obtained for the upper crust. For the lower crust, around 6.5 km/s is computed. Moho located at a depth of about 32 km where P wave velocity is about 7.5 km/s. S wave velocity is around 4.3 km/s at 32 km.

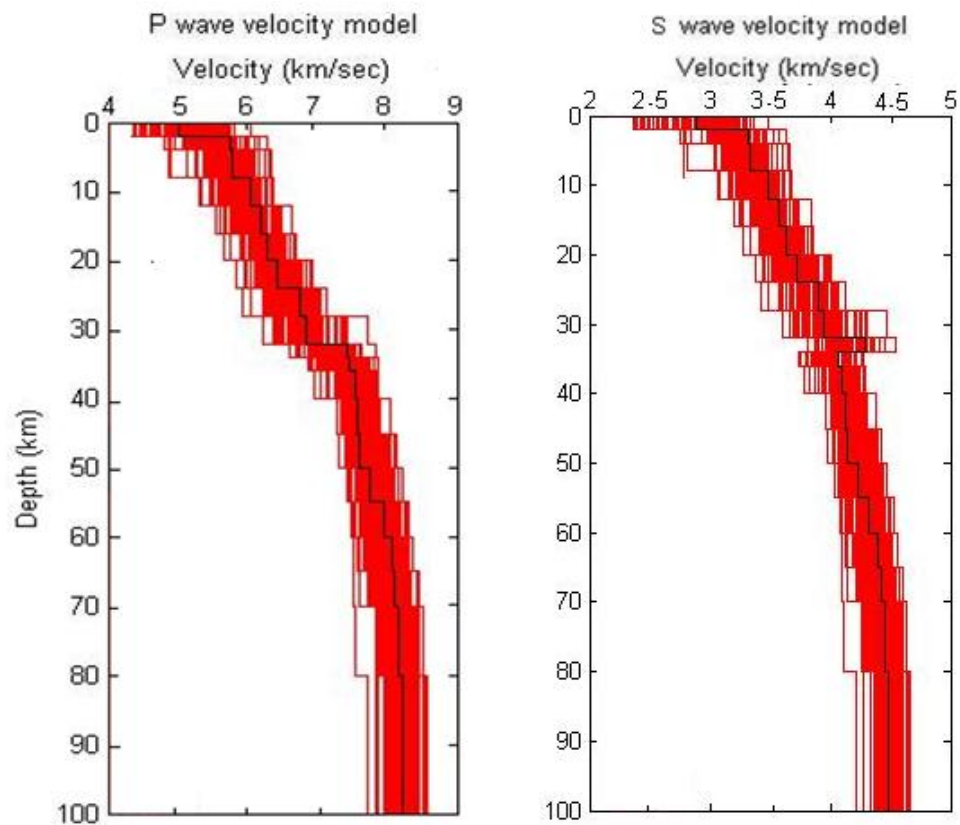


Figure 4.8. P and S wave initial velocity models of the earthquake cluster in sub-region B. Red lines show 100 randomly computed velocity models from an initial model constructed for the region B. The black one shows the initial velocity model for the best final velocity model in Figure 4.9.

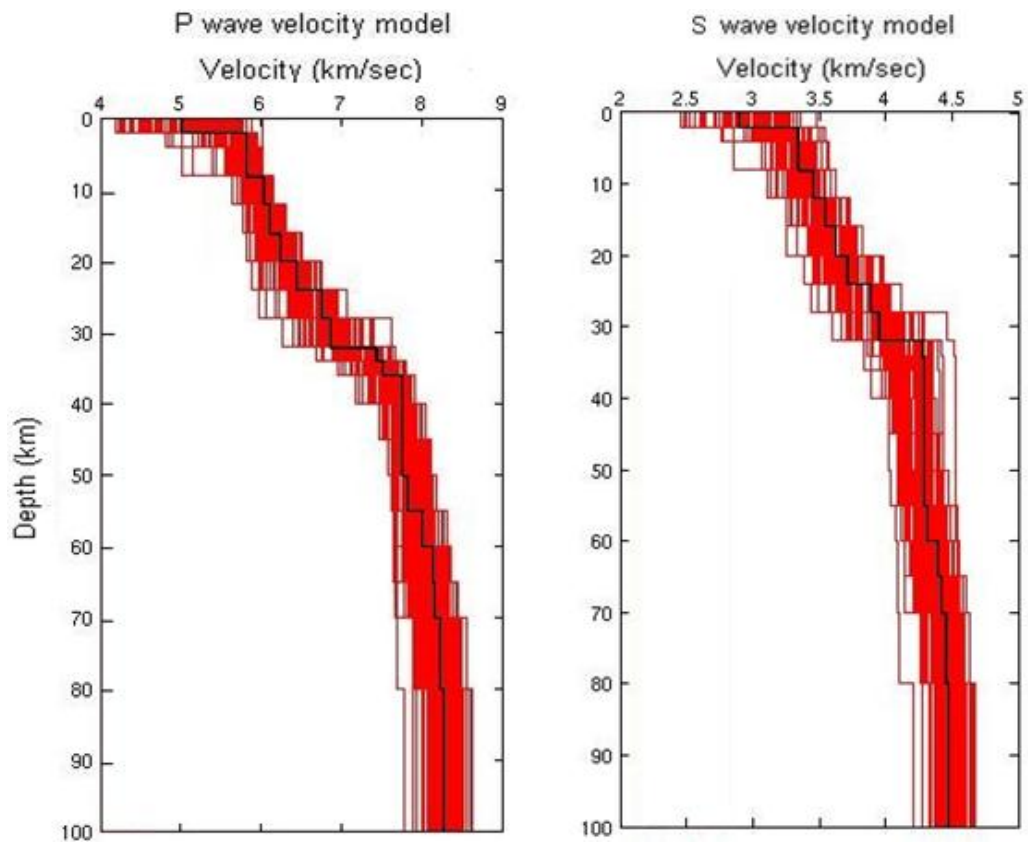


Figure 4.9. P and S wave velocity model of the earthquake cluster in sub-region B. Red lines show 100 final velocity models from the initial model in Figure 4.8. The thick black line shows the best velocity model.

4.2.4. Statistical properties

Mean values of errors of latitude, longitude and depth are 2 km, 2 km and 3 km, respectively (Figure 4.10). All of the events have azimuthal gap, around $90^\circ \pm 60^\circ$. As a result, reliable results are obtained. It can be noticed that most earthquakes occur at the upper crust (~ 10 km). Most of the events are recorded by 10 stations.

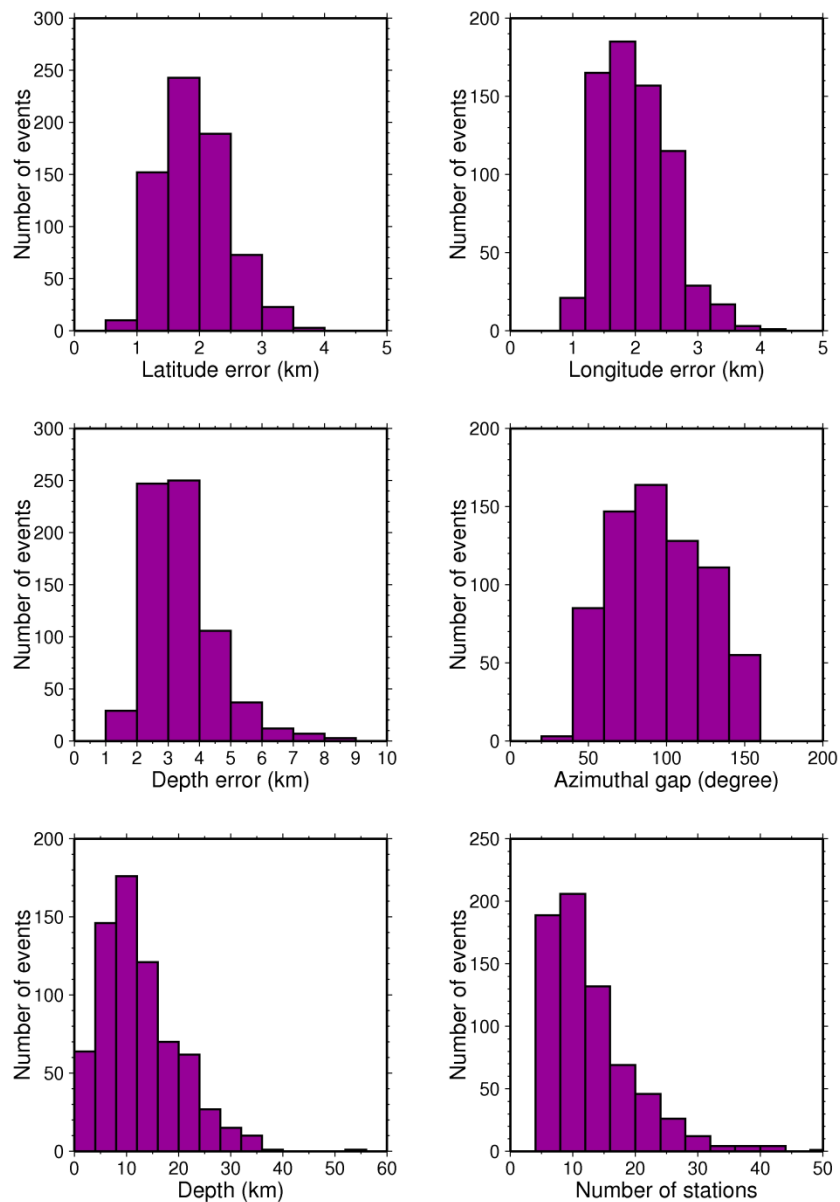


Figure 4.10. Statistics of the catalog for the earthquake cluster in sub-region B.

4.3. Region C: Konya

4.3.1. Hypocentral locations

C presents Konya region (Figure 3.5). More than 700 events were inverted. Total RMS value changed from 0.251 to 0.231. KONT is the reference station (Figure 4.11-inset). Location of the most earthquakes shifted to the south. Many earthquakes happen in the upper and middle crust in this region (hypocentral depth less than 15 km). A small number of events occur below the Moho. Most of the events contain large location errors because of poor station coverage.

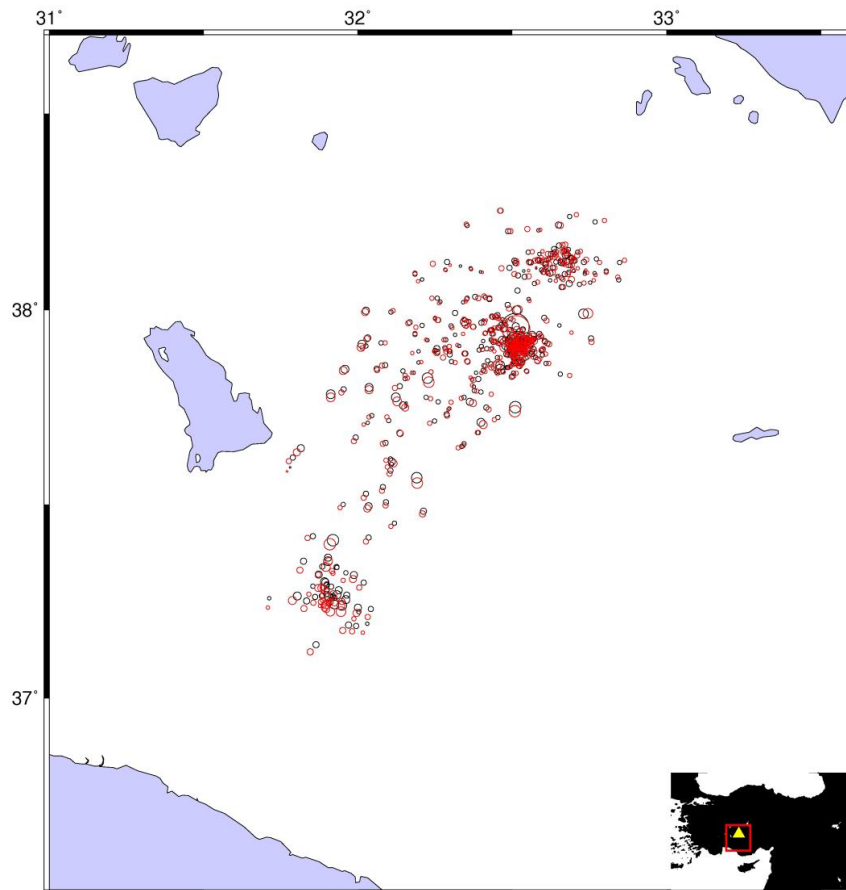


Figure 4.11. Relocated earthquakes for sub-region C. Red circles indicate the earthquakes with the 1D local velocity model obtained from VELEST. Black circles show the earthquakes with initial velocity model. Yellow triangle shows reference station KONT.

4.3.2. Station corrections

Station corrections are displayed in Figure 4.12. Values of the station corrections are presented as relative value with respect to the reference station of KONT (shown with a triangle).

Negative correction values were found for region C which is compatible with the corrections found for cluster B. In region B, positive corrections are obtained, indicating the lower velocities in the crust which is consistent with the results found for cluster A. In region D, station corrections range between 0 and 1 s, which demonstrate lower velocities. It may be related to sediments in Cyprus region. In region E, positive correction values are observed which is consistent with the correction results found for cluster A. Positive corrections are an indication of the presence of lower velocities which may be related to the sediments in Antalya region.

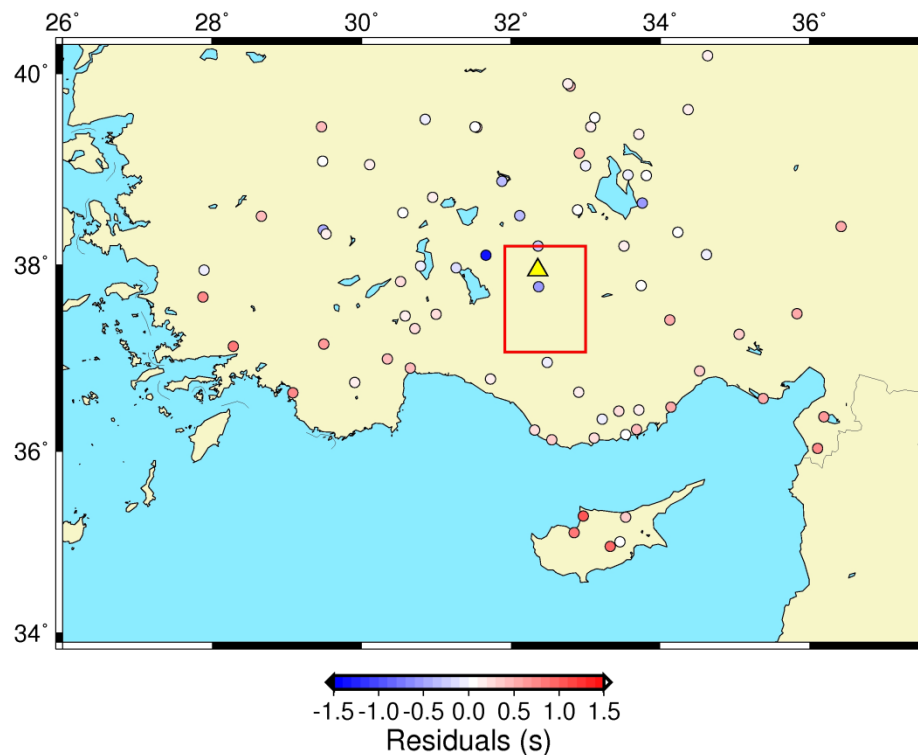


Figure 4.12. Station corrections of the earthquake cluster in sub-region C. Triangle shows the reference station for this cluster.

4.3.3. Velocity model

P wave velocity is around 6 km/s at a depth of 15 km while S wave velocity 3.5 km/s (Figure 4.14). About 6.5 km/s is calculated for P wave in the lower crust. At 32 km, P wave velocity is about 7.5 km/s. The abrupt change from 6.5 to 7.5 km/s apparently indicates the Moho discontinuity. S wave velocity at Moho depth is about 4.3 km/s.

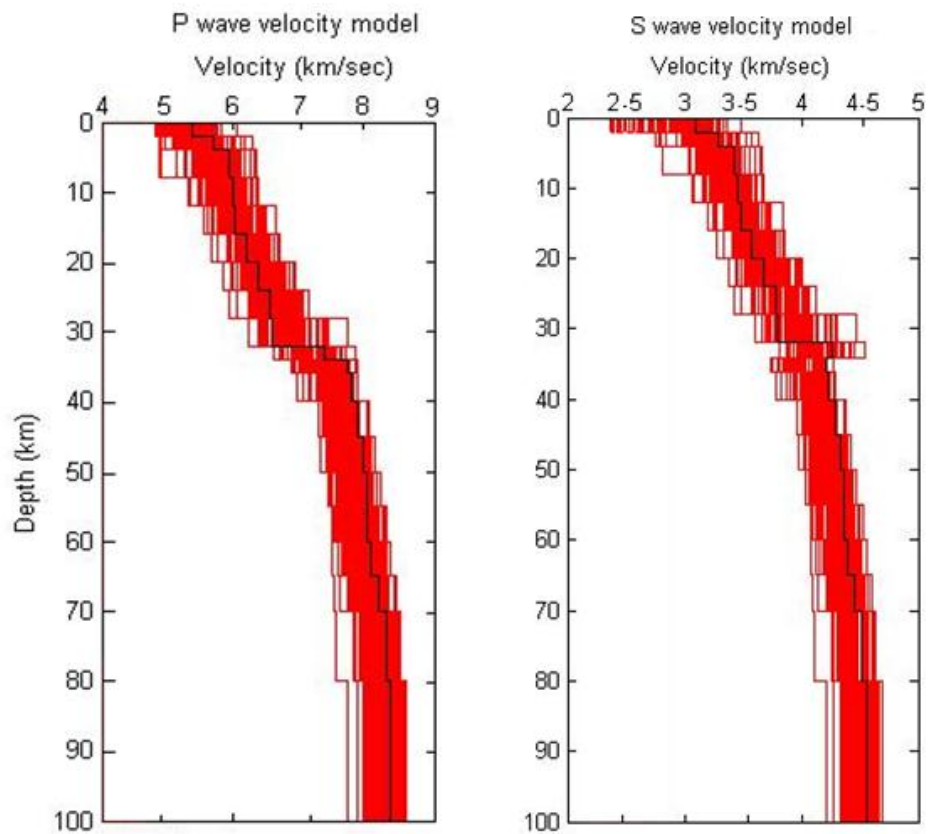


Figure 4.13. P and S wave initial velocity models of the earthquake cluster in sub-region C. Red lines show 100 randomly computed velocity models from an initial model constructed for the region C. The black one shows the initial velocity model for the best final velocity model in Figure 4.14.

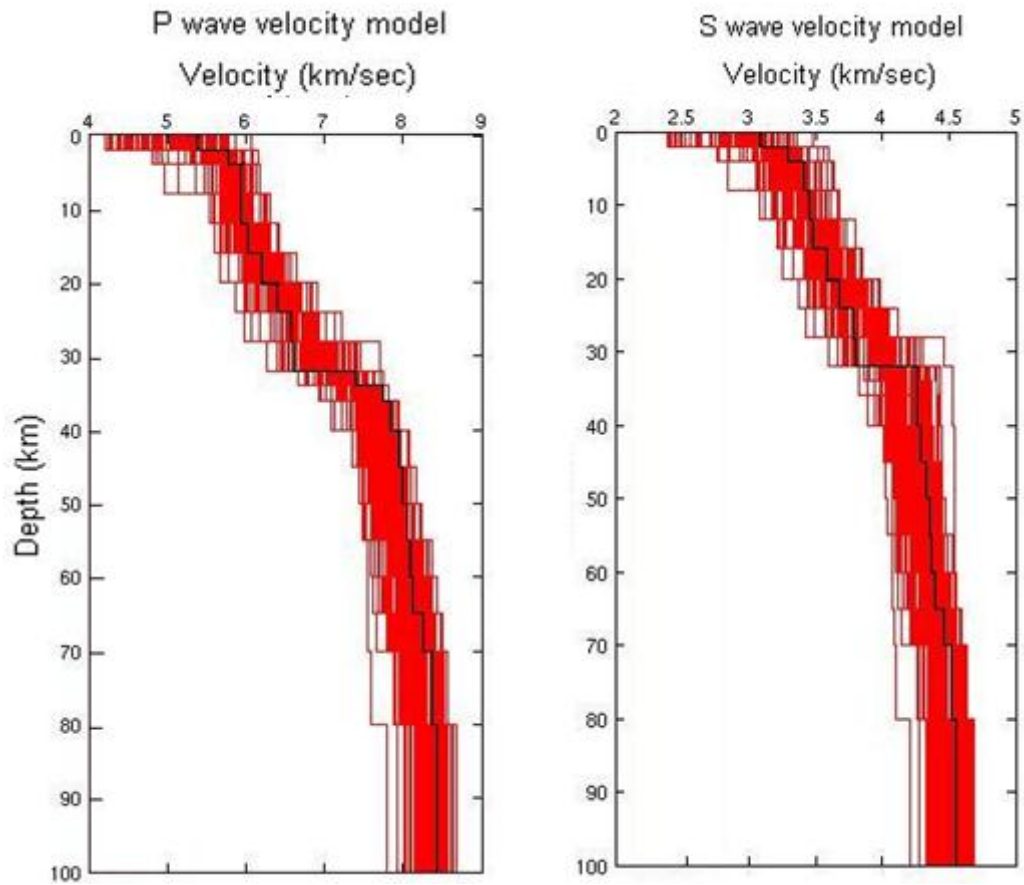


Figure 4.14. P and S wave velocity model of the earthquake cluster in sub-region C. Red lines show 100 final velocity models from the initial model in Figure 4.13. The thick black line shows the best velocity model.

4.3.4. Statistical properties

Most earthquakes in C region have location errors of 2 km for latitude and longitude, 3 km for depth (Figure 4.15). The azimuthal gap does not exceed 220 degrees for the earthquakes in cluster C. Average azimuthal gap is 120 degrees. The depth distribution shows that most of the events are shallower than 25 km. Many earthquakes occur at the upper crust and middle crust. Most of the events are recorded by more than 5 stations.

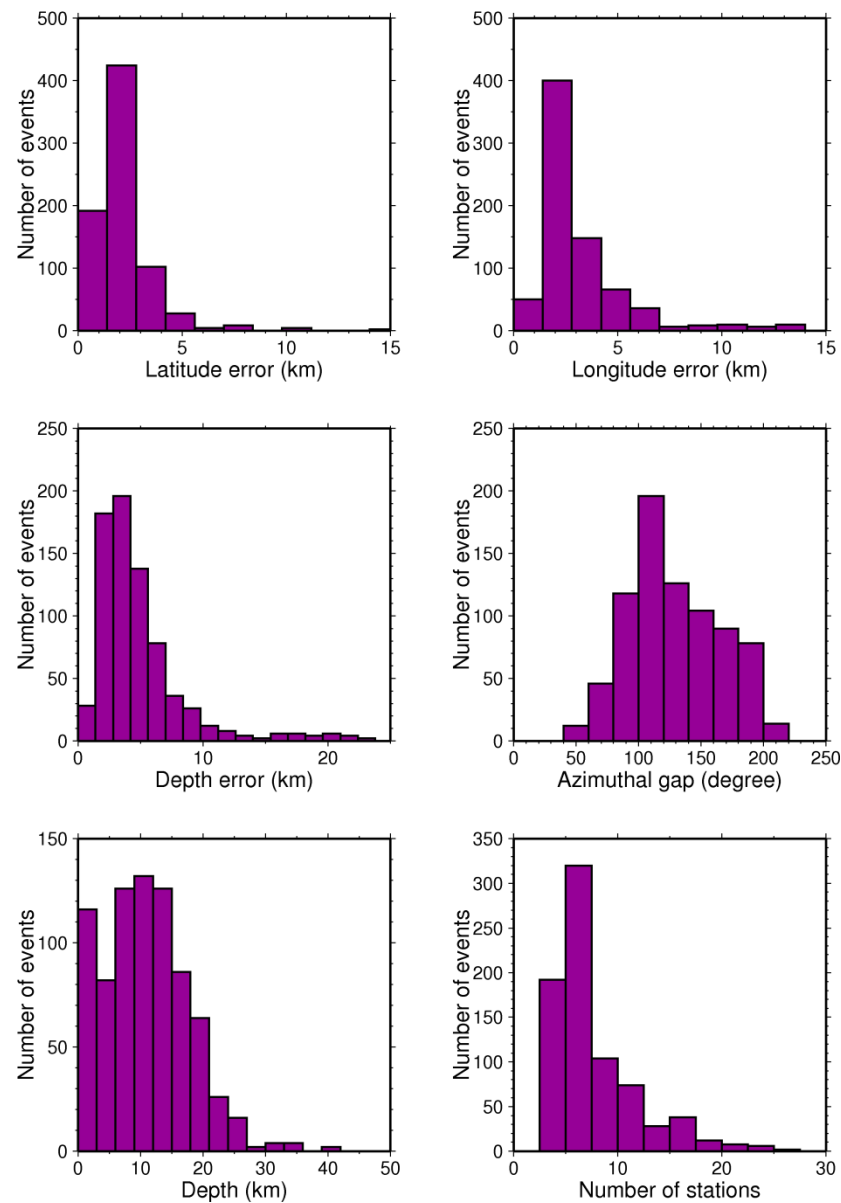


Figure 4.15. Statistics of the catalog for the earthquake cluster in sub-region C.

4.4. Region D: Cyprus

4.4.1. Hypocentral locations

Over 250 events were used for the inversion. Total RMS value reduced from 0.878 to 0.273. CSS is the reference station (Figure 4.16).

Most of earthquake locations are shifted toward the reference station. Most earthquakes occur in the upper crust in this region (hypocentral depth less than 10 km). Many events take place below the Moho. Most of the events are composed of large location errors due to sparse station distribution.

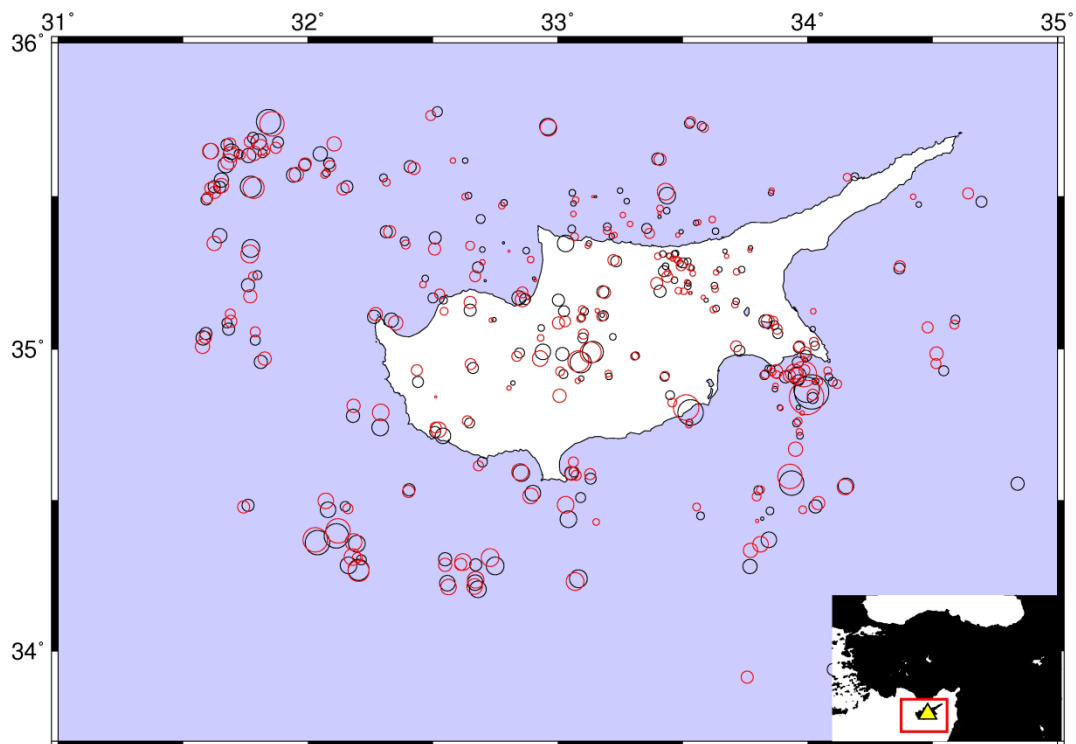


Figure 4.16. Relocated earthquakes for sub-region D. Red circles indicate the earthquakes with the 1D local velocity model obtained from VELEST. Black circles show the earthquakes with initial velocity model. Yellow triangle shows reference station CSS.

4.4.2. Station corrections

The station corrections are calculated as relative to the reference station CSS (Figure 4.17).

Negative corrections were found for region C which is compatible with the results found for cluster B and C. In region B, negative corrections are obtained, indicating higher velocities in the crust which is consistent with the results found for cluster B. In region D, station correction values range between zero and 1.s, which demonstrate lower velocities. It may be related to sediments in Cyprus region. In region A, station corrections have negative values. In general, negative correction values are observed for region E which is consistent with the correction results found for cluster B.

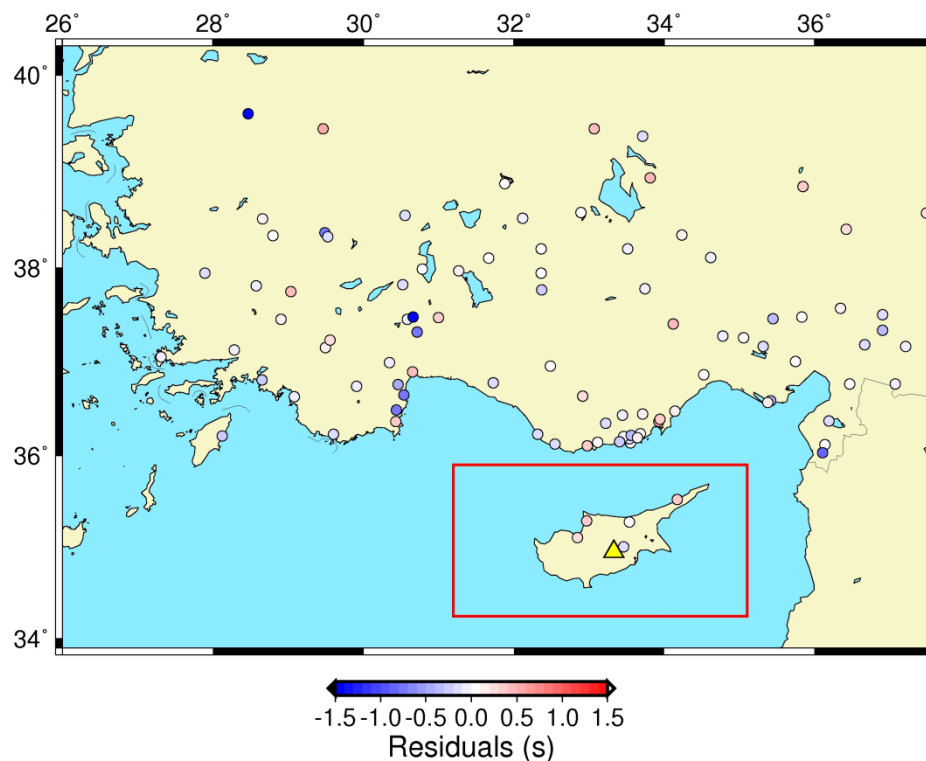


Figure 4.17. Station corrections of the earthquake cluster in sub-region D. Triangle shows the reference station for this cluster.

4.4.3. Velocity model

We noted an increase of velocity with depth. Value about 6.2 km/s is found for the upper crust (Figure 4.19). S wave velocity is 3.5 km/s. For the lower crust, around 6.6 km/s is obtained at a depth of 20 km. At 30 km, P wave velocity is about 7.5 km/s while S wave velocity is 4.4 km/s. The change from 7 to 7.5 km/s may indicate the Moho discontinuity.

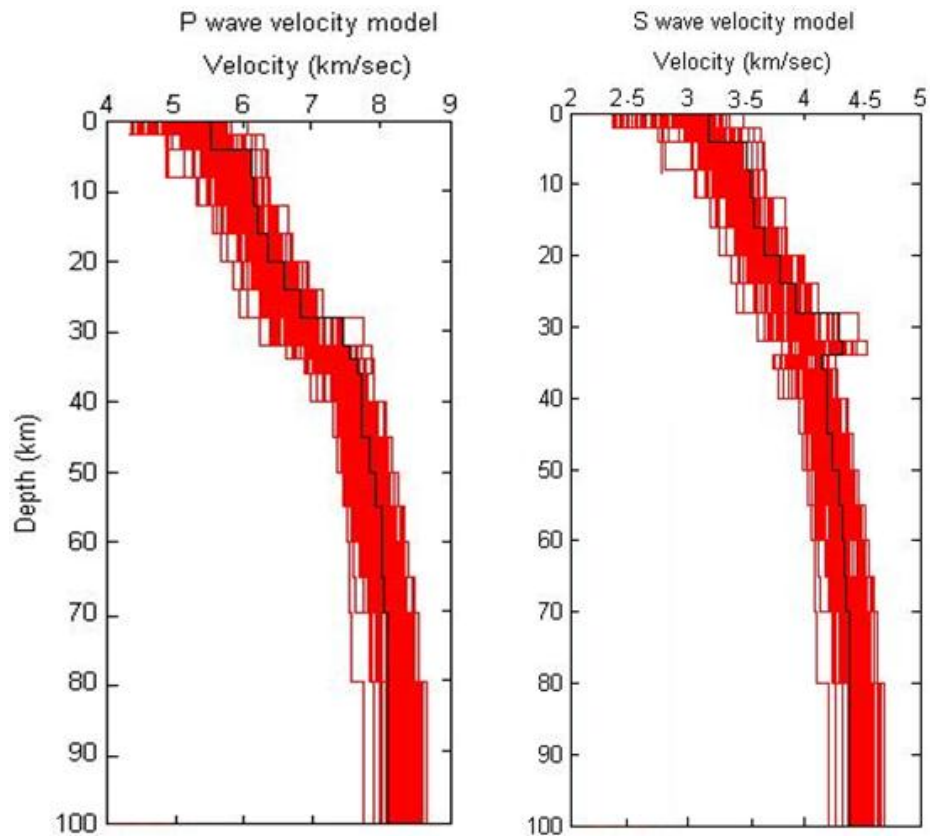


Figure 4.18. P and S wave initial velocity models of the earthquake cluster in sub-region D. Red lines show 100 randomly computed velocity models from an initial model constructed for the region D. The black one shows the initial velocity model for the best final velocity model in Figure 4.19.

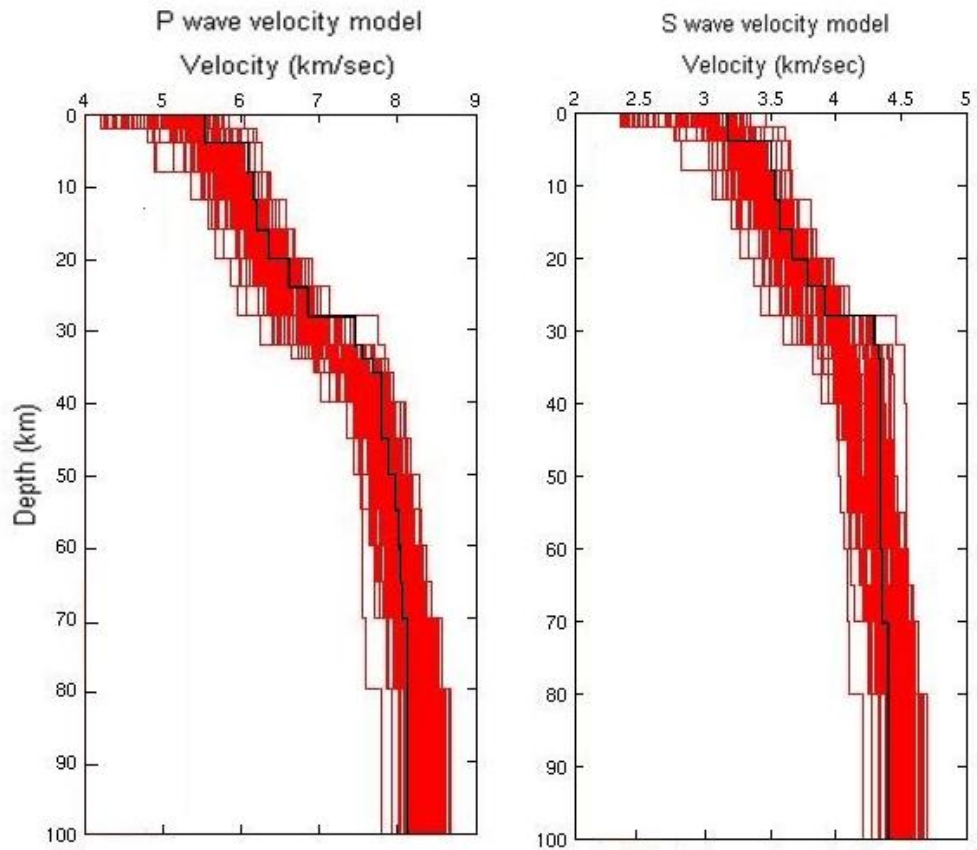


Figure 4.19. P and S wave velocity model of the earthquake cluster in sub-region D. Red lines show 100 final velocity models from the initial model in Figure 4.18. The thick black line shows the best velocity model.

4.4.4. Statistical properties

Most of the events in D region contain higher location errors (Figure 4.20). Average errors are 5 km for latitude and longitude, 7 km for depth. Average azimuthal gap is 250 degree for most of the earthquakes. Earthquake locations in which the azimuthal gap exceeds 180 degrees typically have large horizontal and depth error values. Most events occur in the upper and lower crust. There are also earthquakes which happen upper mantle. Most of the events are recorded by five stations.

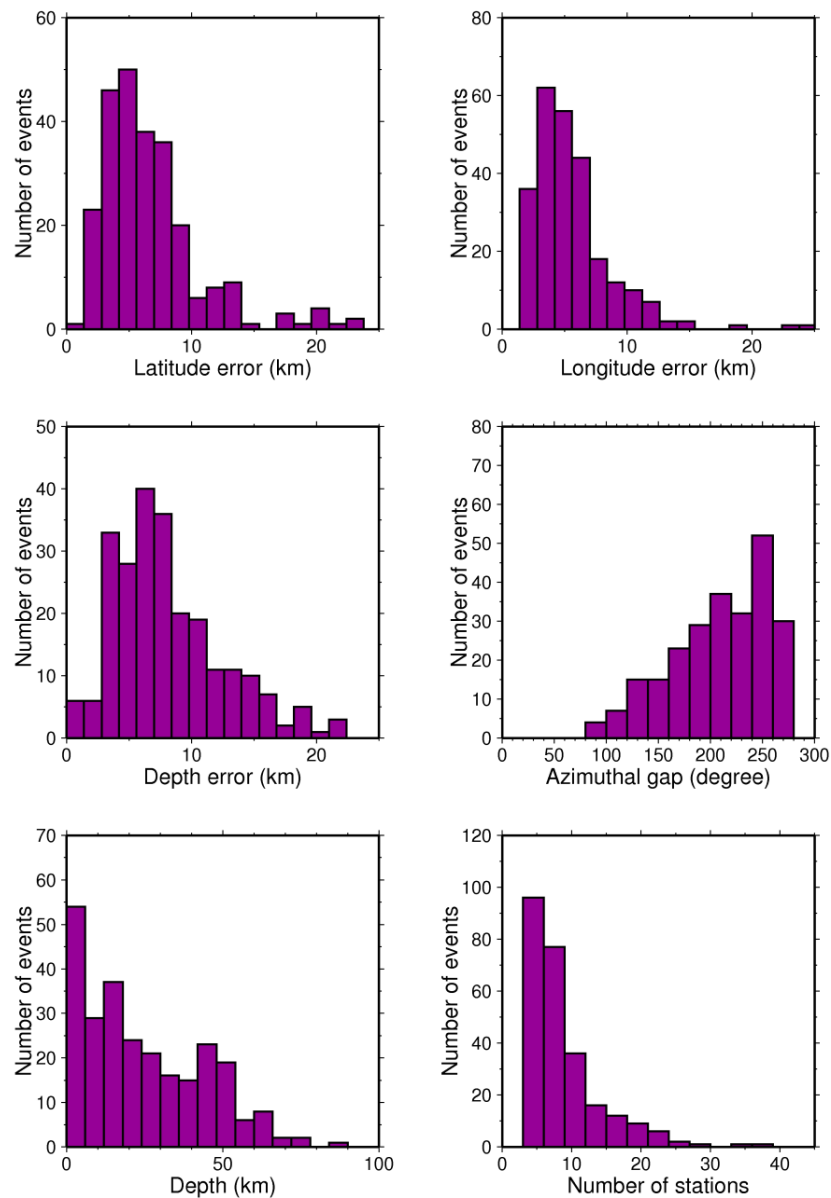


Figure 4.20. Statistics of the catalog for the earthquake cluster in sub-region D.

4.5. Region E: Antalya

4.5.1. Hypocentral locations

Antalya region is classified as E in Figure 3.5. Over 300 events were employed for the analysis. Decrease in the total rms value is from 0.331 to 0.273. ANTB is the reference station (Figure 4.21-inset).

Most hypocenter locations of the events changed toward southwest. Most of events in region E occur in the upper crust. (hypocentral depth about 5 km). A significant number of events occur in the upper mantle. Deep earthquakes occur in Antalya bay. Deep earthquakes are fundamental to enhance the seismotectonics of the region E.

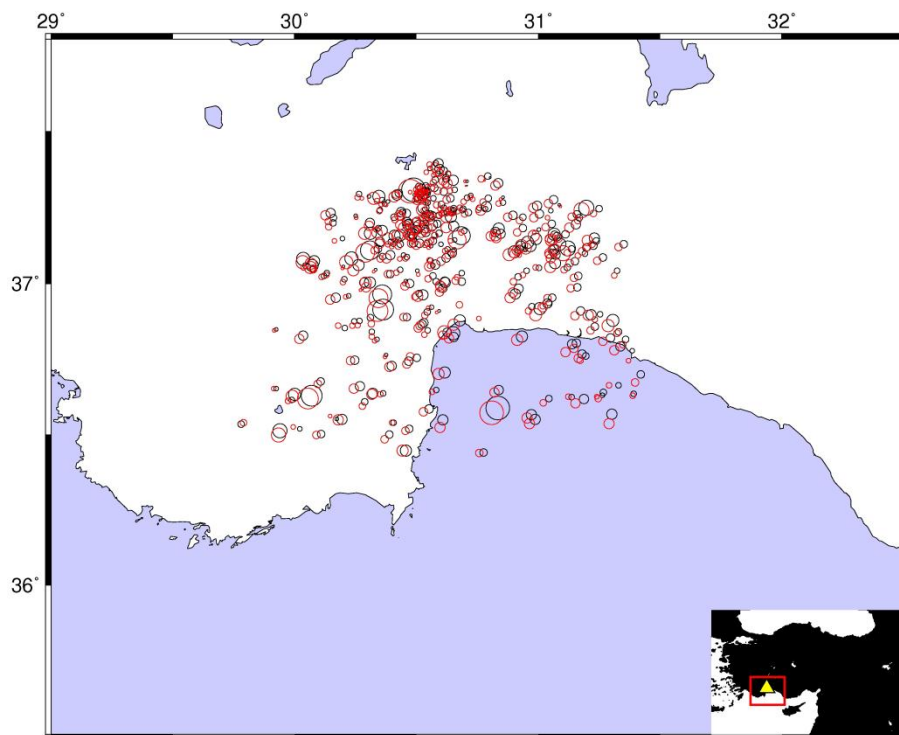


Figure 4.21. Relocated earthquakes for sub-region E. Red circles indicate the earthquakes with the 1D local velocity model obtained from VELEST. Black circles show the earthquakes with initial velocity model. Yellow triangle shows reference station ANTB.

4.5.2. Station corrections

In Figure 4.22, station corrections are presented. The station corrections are calculated relative to the reference station of ANTB.

Negative correction values were obtained for region A. In region B, positive correction values are observed which indicate the lower velocities in the crust which is consistent with the results found for cluster A. The lower velocities may be related to the sediments in Adana basin. In region C, station correction values range between -0.5 and -1 s. which demonstrate higher velocities. The results in region C is compatible with the correction results found for cluster B, C and D. In region D, negative values found which demonstrate high velocities. The results are also consistent with the results found for cluster A and B. Negative correction values also obtained for the region E which is also compatible with cluster B and D.

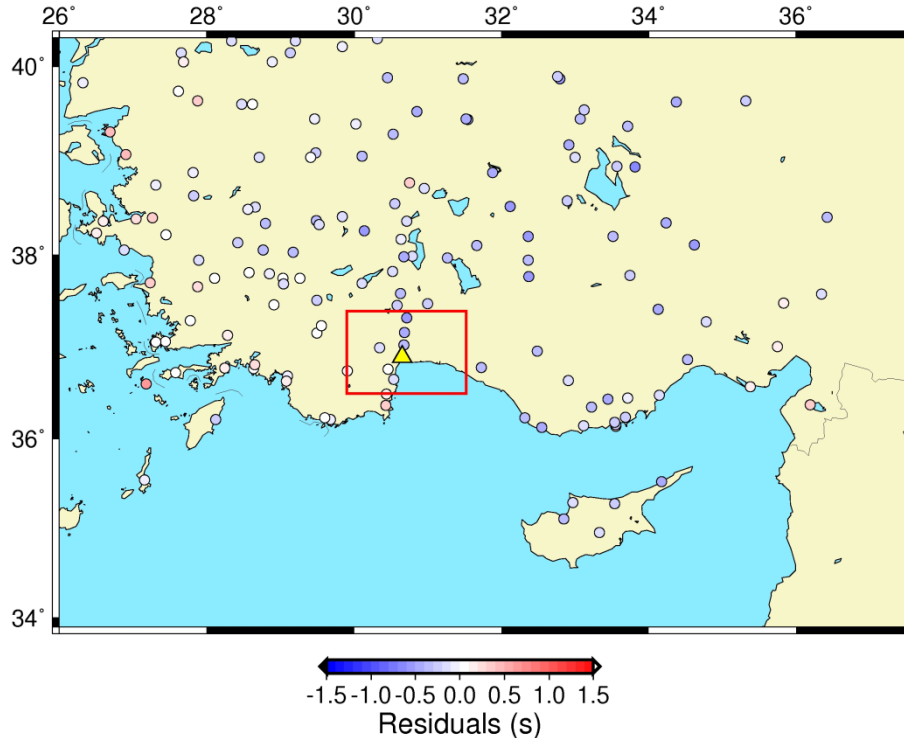


Figure 4.22. Station corrections of the earthquake cluster in sub-region E. Triangle shows the reference station for this cluster.

4.5.3. Velocity model

At 12 km, value around 5.8 km/s is calculated (Figure 4.24). S wave velocity is 3.5 km/s in the upper crust. At 20 km, about 6.5 km/s is obtained. S wave velocity is 3.7 km/s for lower crust. At Moho depth, P wave velocity is about 7.5 km/s while S wave is 4.4 km/s.

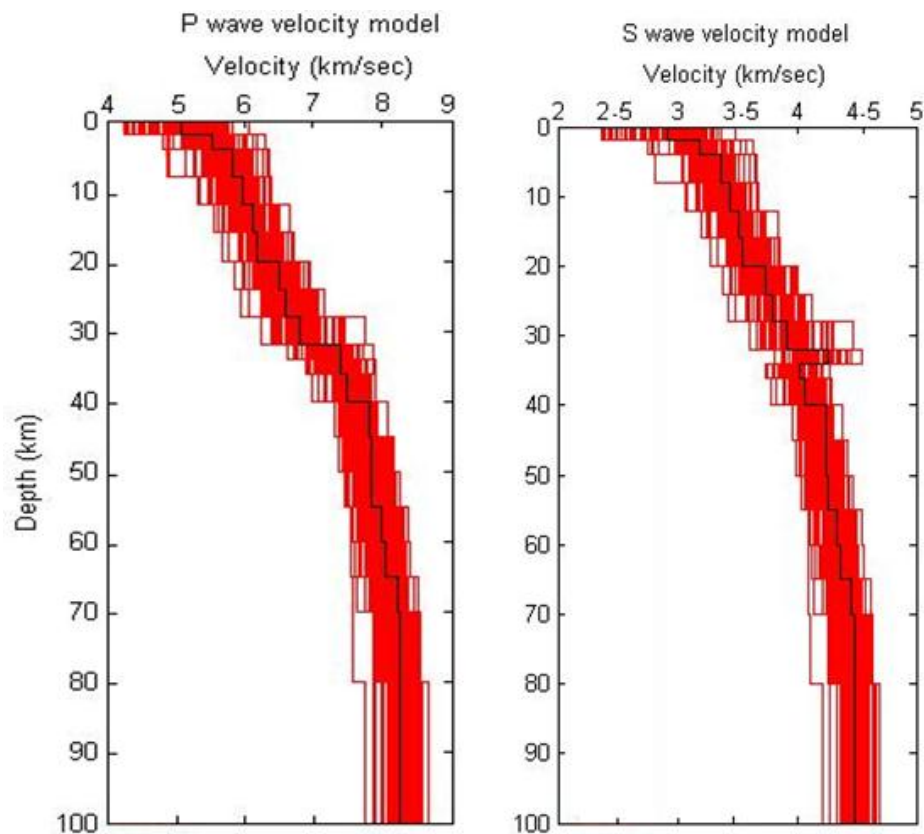


Figure 4.23. P and S wave initial velocity models of the earthquake cluster in sub-region E. Red lines show 100 randomly computed velocity models from an initial model constructed for the region E. The black one shows the initial velocity model for the best final velocity model in Figure 4.24.

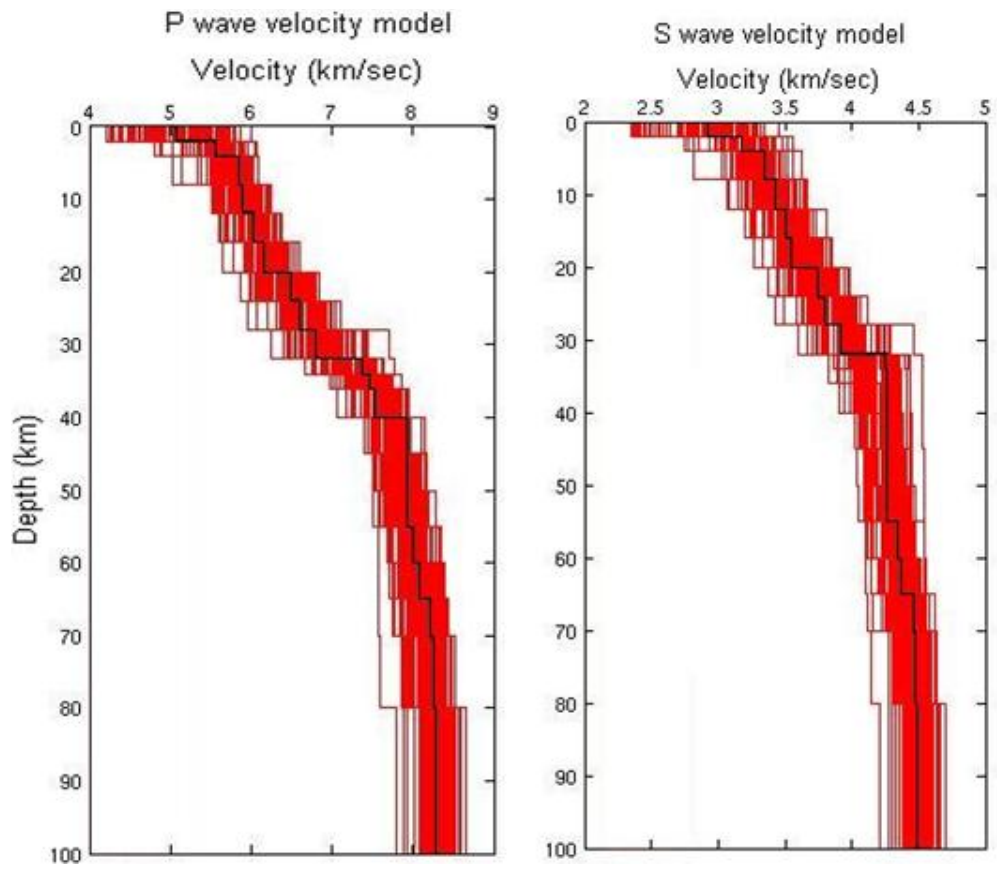


Figure 4.24. P and S wave velocity model of the earthquake cluster in sub-region E. Red lines show 100 final velocity models from the initial model in Figure 4.13. The thick black line shows the best velocity model.

4.5.4. Statistical properties

Average location errors are 2 km, 2 km and 5 km for latitude, longitude and depth, respectively (Figure 4.25). Average azimuthal gap is 100 degrees. The depth distribution indicates that most of the events in region A are shallower than 30 km. Most earthquakes occur in the upper crust while there are a significant number of events which happen in the upper mantle. The deepest earthquake in region E occur at the depth of 132 km. Most of the events are recorded by 10 stations.

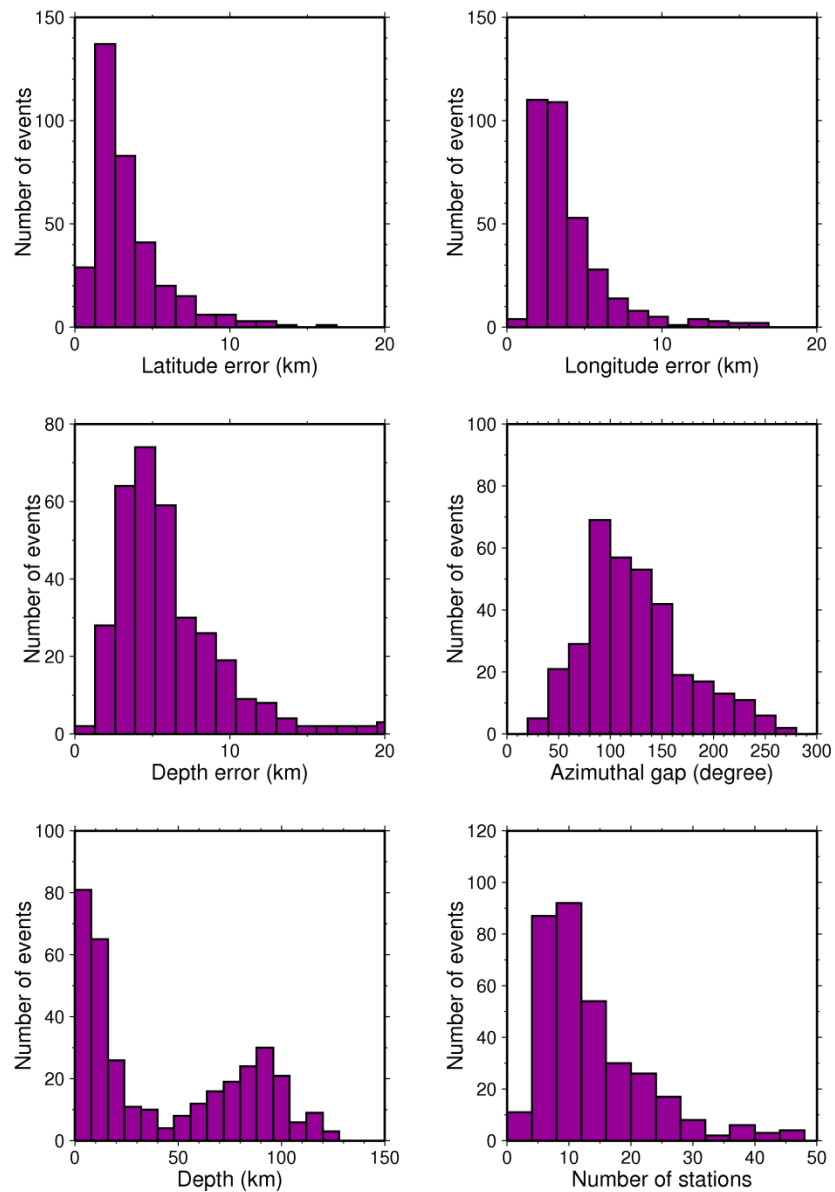


Figure 4.25. Statistics of the catalog for the earthquake cluster in sub-region E.

4.6. Overall Velocity Profiles

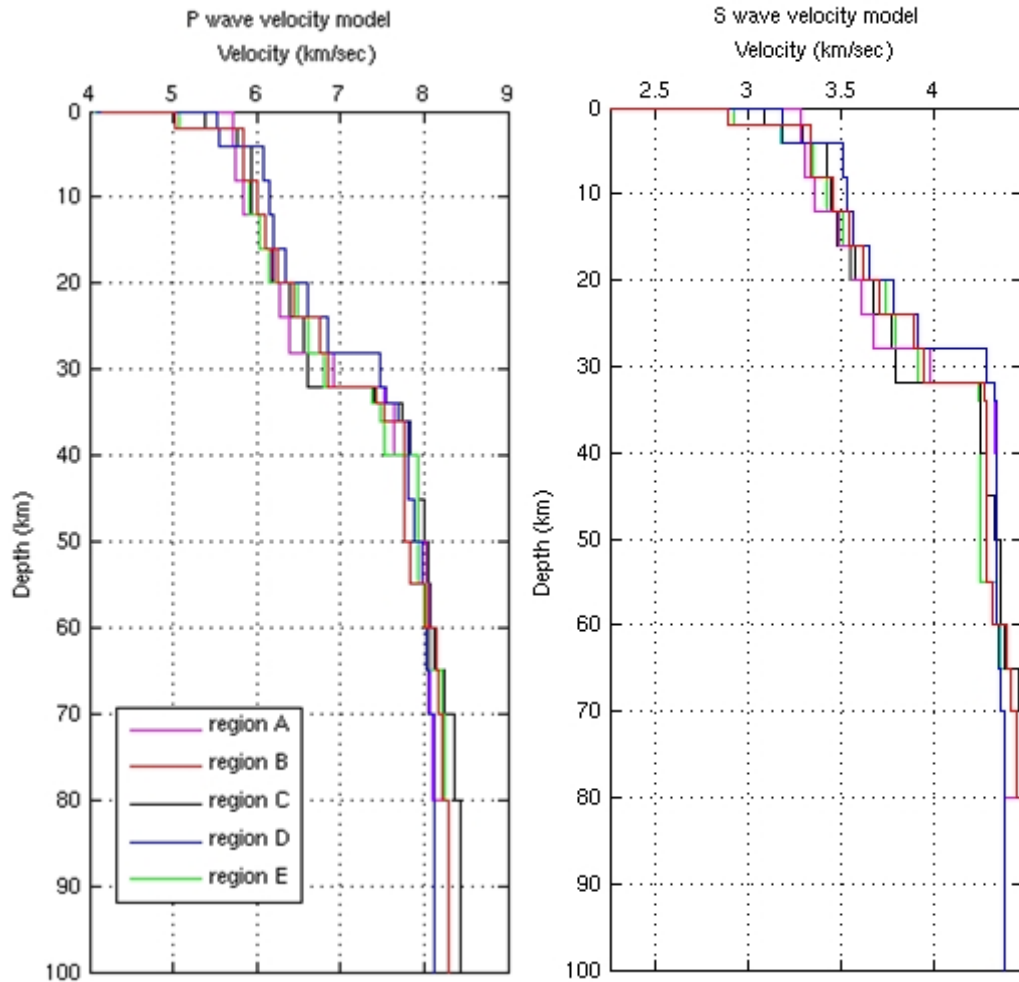


Figure 4.26. Final P and S velocity models for all clusters

What we find significant here is that all five, quite distinct sub-regions (clusters), show consistent P and S velocity profiles and Moho depth. It can be noticed that Moho depth at southern Turkey is around 32 km. Furthermore, low velocities are observed in region B and E in shallower parts (~ 3-5 km range). In region B, low P and S velocities may be related to the sedimentary sequences in the Adana basin. Whereas in region E, low velocities may be correlated with shallow young sediments in Antalya basin.

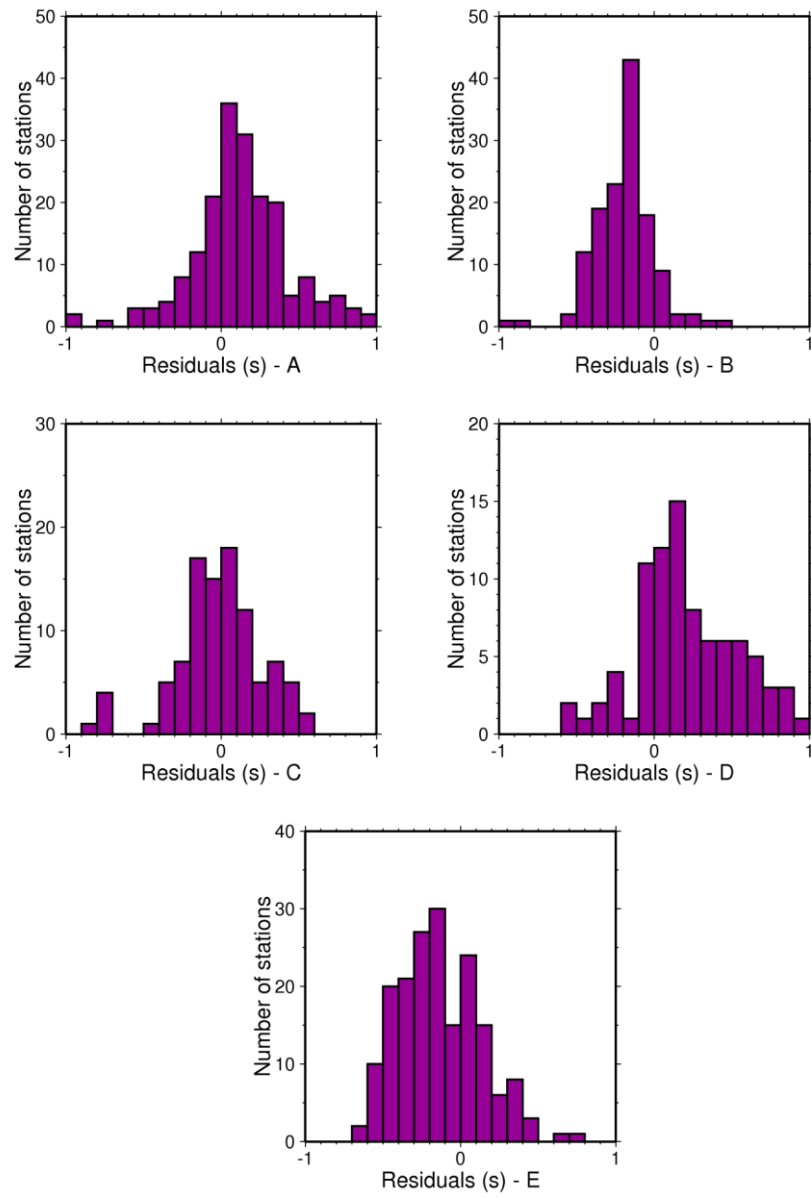


Figure 4.27. Station corrections for all regions

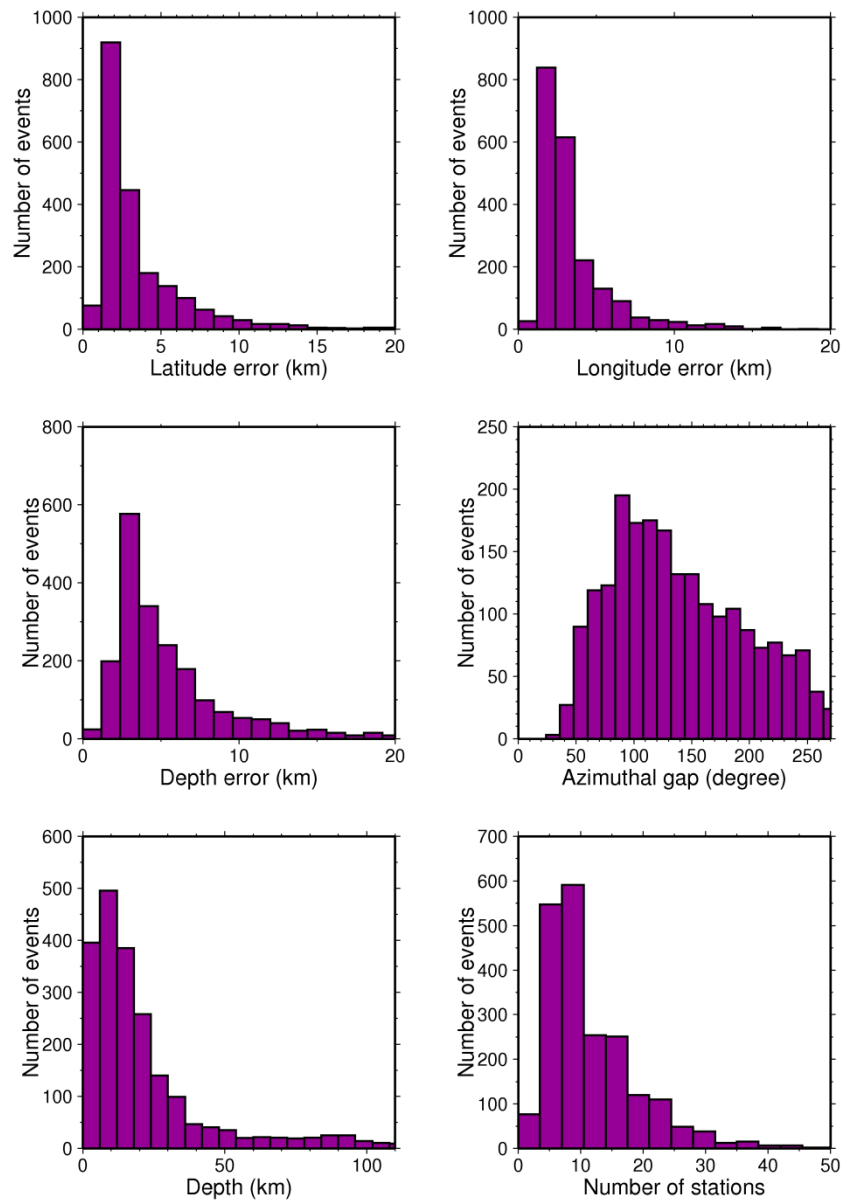


Figure 4.28. The statistics of the catalog with the locations computed using the 1D velocity models estimated from the VELEST.

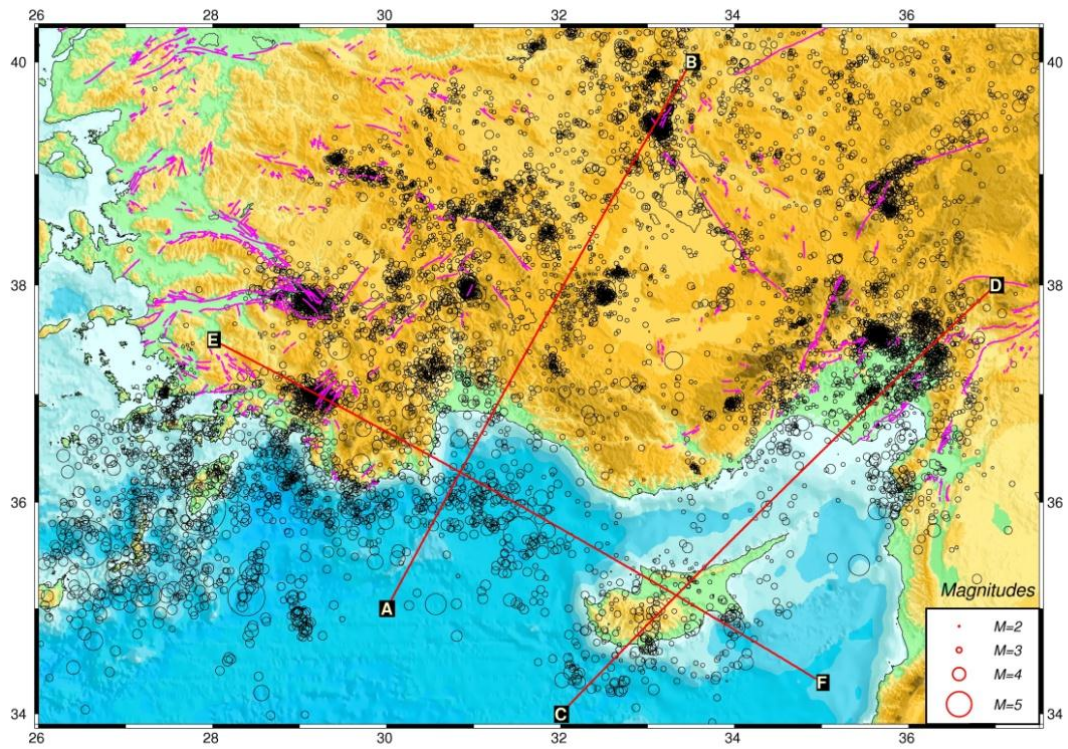


Figure 4.29. Earthquakes which are relocated with 1-D velocity models and station corrections. Red lines show the profiles for cross-sections in Figure 4.30.

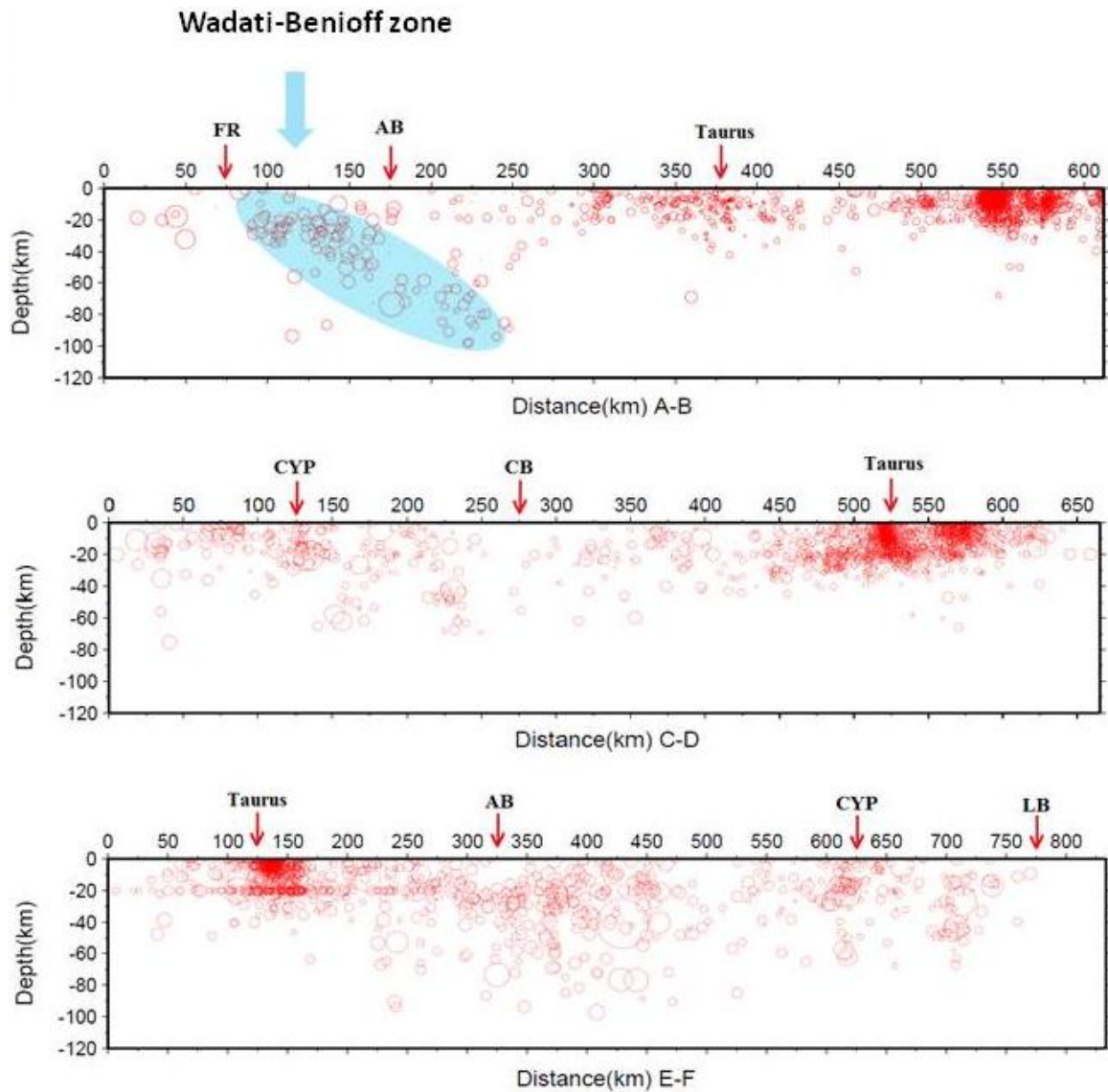


Figure 4.30. Cross section views of earthquake hypocenters. Letters above are explained in Figure 1.1.

We present cross section plots in depth across various parts of the Cyprian Arc (Figure 4.30). It can be noticed that cross-section plot along A-B, the deep earthquakes occur under Antalya Basin. However, most of the earthquakes take place 20 km under Taurus platform. There are almost no events under the Florence Rise, this gap may signify low strain in this area. A descending pattern of earthquakes along Antalya Basin is observed. This may be suggestive of subducted slab.

Along C-D cross-section plot; under Cyprus, most of the events occur at a depth of 25 km while under Taurus, the depth of the earthquakes rarely exceeds 40 km. Under the Cilicia Basin, almost no hypocenters are observed. This may also indicate no strain in the area.

Along E-F cross-section plot; under Taurus platform, most events happen in the upper crust. Red circles indicate located hypocenters occur at depths greater than 40 km under Cyprus. It is also observed that deep earthquakes are nucleated under Antalya Basin. There is an earthquake sequence at 20 km. This may be due to either the poor S phase readings or bad readings in the data-set.

5. DISCUSSIONS

We computed a one-dimensional (1D) velocity models and station corrections in Cyprus subduction zone and Southern Turkey. Using these velocity models, we relocated earthquakes during 2005-2011 (Figure 3.5). For five regions, total RMS values of earthquakes are decreased significantly. The total RMS value of all events (0.158 s.) exhibits a significant reduction with respect to the initial earthquake locations (0.348 s.) (Figure 4.29).

The station corrections are calculated relative to the reference stations of five clusters. Station corrections of region B, C, D and E, positive correction values show lower velocities in the regions. Lower velocity may show sediments in Adana Basin. Lower velocity in region C, may also indicate a thick sediment pile in Konya region. Furthermore, in region E, it may be linked with shallow sediments in Antalya Basin. In region D, it may be related to sediments in Cyprus region.

Moho depth at southern Turkey is around 32 km and quite consistent for all the models presented (Figure 4.26). The result is consistent with the results of tomographic study of Koulakov and Sobolev (2006). Koulakov and Sobolev (2006) observed Moho depth beneath Cyprus as 33 km. Makris *et al.* (1983) computed Moho depth as 35 km. Moho depth is varying from 30 km to 35 km beneath the Eastern Mediterranean (Tesauro *et al.*, 2007). However, the Moho depth is about 38 km underneath Antalya Basin. The values obtained in our study are quite lower. According to Mutlu and Karabulut (2011), large crustal thicknesses are obtained along the southern coast of Turkey (40-48 km). Grad *et al.* (2009) calculated Moho depth that is varying from 30 km to 35 km beneath southern coast of Turkey and Cyprus. However, there is poor coverage of the data set in the eastern Mediterranean. Moreover, Bassin *et al.* (2000) obtained Moho depth beneath Adana and Konya region as 40 km. The Moho depth is between 30-35 km in Fethiye and Antalya region while 25 km beneath Cyprus in the global crustal model, Crust 2.0 (Bassin *et al.*, 2000).

Low velocities are obtained in region B and E at a depth of about 3-5 km. In region B, low P and S velocities may be related to the sedimentary sequences in Adana Basin,

while in region E, it may be linked with shallow young sediments in Antalya Basin (Figure 4.26).

Cross-section plots suggest that the deep earthquakes (~100 km) occur under Antalya Basin. A well-defined Wadati-Benioff zone can be identified in the top panel of Figure 4.30, corresponding to Antalya basin extending to about 100 km depth. Previous seismic tomography studies have also resolved a subducting slab underneath the Anatolia (Spakman *et al.*, 1991; Bijwaard *et al.*, 1998; Piromallo and Morelli, 2003; Biryol *et al.*, 2011). Under Taurus platform, most of the events occur in the upper crust (Figure 4.30).

6. CONCLUSIONS

In this study, 1D local crustal structures in Cyprus subduction zone and southern Turkey are presented. A reference 1D models and station corrections are derived for a selected data-set, according to the procedure described by Kissling *et al.* (1995).

A consistent decrease of travel time residuals between previous earthquake locations and new relocated events displays more accurate hypocenter locations. By employing the new model, the new locations are close enough to the real locations (Figure 4.29).

Station corrections provide essential information to improve the resolution of the shallow part of the crustal structure. Station corrections display variations that are related to the surface geology. In this study, the patterns of the station corrections are consistent with surface geology observations.

The discontinuous jump of P and S velocities at about 32 km roughly indicates the average Moho depth for our clusters which is compatible with the crustal models of Tesauro *et al.* (2007) and Grad *et al.* (2009). Moho depth value of global crustal model, Crust 2.0 (Bassin *et al.*, 2000) is also consistent with results of Antalya and Fethiye region in our study. Furthermore, the result of tomographic study of Koulakov and Sobolev (2006) is consistent with obtained Moho depth. Region B and E, which is characterized by low P and S velocities in shallower parts (~ 3-5km), correlates well with the sedimentary sequences in the Adana basin and young sediments in Antalya Basin (Figure 4.26).

Our conclusions on Minimum 1D velocity model of southern Turkey will contribute to perform local earthquake tomography. Minimum 1D velocity model represents an improvement for earthquake location superior to any 1D velocity model based on actual a-priori information of southern Turkey. Our model represents a first step towards more detailed seismic studies.

REFERENCES

- Aktar, M., M. Ergin, S. Özalaybey, C. Tapırdamaz, A. Yörük and F. Biçmen, 2000, “A lower-crustal event in the northeastern Mediterranean: the 1998 Adana Earthquake ($M_w = 6.2$) and its aftershocks”, *Geophysical Research Letters*, Vol. 27, pp. 2361–2364.
- Aksu A. E., J. Hall and C. Yaltrak, 2009, “Miocene-Recent evolution of Anaximander Mountains and Finike Basin at the junction of Hellenic and Cyprus Arcs, eastern Mediterranean”, *Marine Geology*, Vol. 258, pp. 24-47.
- Arvidsson, R., Z. Ben-Avraham, Z., G. Eckström and S. Wdowinski, 1998, “Plate tectonic framework for the October 9, 1996 Cyprus earthquake”, *Geophysical Research Letters*, Vol. 25, pp. 2241–2244.
- Asch, C., N. Chamot-Rooke and M. Pubellier, 2004, IGME 5000: International Geological Map of Europe and Adjacent Areas, *IGME – Commission for the Geological Map of the World (CGMW)*.
- Bassin, C., G. Laske and G. Masters, 2000, “The current limits of resolution for surface wave tomography in North America”, *Eos Trans American Geophysical Union*, Vol. 81, F897.
- Ben-Avraham, Z. and A. Ginzburg, 1990, “Displaced terranes and crustal evolution of the Levant and the eastern Mediterranean”, *Tectonics*, Vol. 9, pp. 613–622.
- Ben-Avraham, Z., A. Ginzburg, J. Makris and L. Eppelbaum, 2002, “Crustal structure of the Levant Basin, eastern Mediterranean”, *Tectonophysics*, Vol. 346, pp. 23-43.
- Bijwaard, H., W. Spakman and R. Engdahl, 1998. “Closing the gap between regional and global travel time tomography”, *Journal of Geophysical Research*, Vol. 103, pp. 30055–30078.

- Biryol, C. B., S. L. Beck, G. Zandt and A. A. Özacar, 2011, “Segmented African Lithosphere Beneath the Anatolian Region Inferred from Teleseismic P-Wave Tomography”, *Geophysical Journal International*, Vol. 184, pp. 1037–1057.
- Boschi L., G. Ekström and K. Kustowski, 2004, “Multiple resolution surface wave tomography: the Mediterranean Basin”, *Geophysical Journal International*, Vol. 157, pp. 293-304.
- Dercourt, J., L. P. Zonenshain, L. E. Ricou, X. Le Pichon, A. L. Knipper, C. Grandjaquet, I. M. Sbertshikov, J. Geussant, C. Lepvrier, D. H. Pechersku, J. Boulin, M. L. Bazhenov, J. P. Lauer and B. Biju-Duval, 1986, “Geological evolution of the Tethys belt from the Atlantic to the Pamirs since the Lias”, *Tectonophysics*, Vol. 123, pp. 241–315.
- Dewey, J. F., W.C. Pitman, W. B. F. Ryan and J. Bonnin, 1973, “Plate tectonics and the evolution of the Alpine system”, *Geological Society of America Bulletin*, Vol. 84, pp. 3137-3150.
- Dewey, J. F., M. R. Hempton, W. S. F. Kidd, F. Şaroğlu, and A. M. C. Şengör, 1986, “Shortening of continental lithosphere: The neotectonics of eastern Anatolia—a young collision zone”, in *Collision Tectonics*, edited by M. P. Coward and A. C. Ries, *Geological Society Special Publications*, Vol. 19, pp. 3-36.
- Dewey J.F., 1988, “Extensional collapse of orogens”, *Tectonics*, Vol. 7, pp. 1123-1139.
- Dewey, J.F., M. L. Helman, E. Turco, D. H. W. Hutton and S. D. Knott, 1989, “Kinematics of the western Mediterranean”, in *Alpine Tectonics*, edited by M. P. Coward, D. Detrich and R. G. Park, *Geological Society London Special Publication*, Vol. 45, pp. 265–283.
- Ergün M., S. Okay, C. Sarı, E. Z. Oral, M. Ash, J. Hall and H. Miller, 2005, “Gravity anomalies of the Cyprus Arc and their tectonic implications”, *Marine Geology*, Vol. 221, pp. 349-358.

- Garfunkel, Z. and B. Derin, 1985, "Permian–early Mesozoic tectonism and continental margin formation in Israel and its implications of the history of the eastern Mediterranean", *Geological Society of London*, Vol. 17, pp. 187–201.
- Garfunkel, Z., 1998, "Constraints on the origin and history of the Eastern Mediterranean basin", *Tectonophysics*, Vol. 298, pp. 5–35.
- Ginzburg, A. and Z. Ben-Avraham, 1987, "The deep structure of the Levant continental margin", *Annales Tectonicae*, 1, pp. 105-115.
- Grad, M., T. Tiira and ESC Working Group, 2009, "The Moho depth map of the European Plate", *Geophysical Journal International*, Vol. 176, pp. 279-292.
- Jolivet L. and C. Faccenna, 2000, "Mediterranean extension and the Africa-Eurasia collision", *Tectonics*, Vol. 19, pp. 1095-1106.
- Karakaya, N., M. Ç. Karakaya, A. Temel, Ş. Küpeli and C. Tunoğlu, 2004, "Mineralogical and chemical characterization of sepiolite occurrences at Karapınar (Konya Basin, Turkey) ", *Clays and Clay Minerals*, Vol. 52, pp. 495-509.
- Khair, K. and G. N. Tsokas, 1999, "Nature of the Levantine (eastern Mediterranean) crust from multiple-source Werner deconvolution of Bouguer gravity anomalies", *Journal of Geophysical Research*, Vol. 104, pp. 25469-25478.
- Kissling E., 1988, "Geotomography with local earthquake data". *Reviews of Geophysics.*, Vol. 26, pp. 659–698.
- Kissling, E., W. L. Ellsworth, D. Eberhart-Phillips and U. Kradolfer, 1994, "Initial Reference Models in Local Earthquake Tomography", *Journal of Geophysical Research*, Vol. 99 (B10), pp. 19635–19646.
- Kissling E., 1995, "Velest User's Guide", *Technical report*, Institute of Geophysics, ETH Zurich, Switzerland.

- Koulakov, I. and S. V. Sobolev, 2006, “Moho depth and three-dimensional P and S structure of the crust and uppermost mantle in the Eastern Mediterranean and Middle East derived from tomographic inversion of local ISC data”, *Geophysical Journal International*, Vol. 164, pp. 218-235.
- Kustowski B., G. Ekström and A. M. Dziewonski, 2008, “The shear-wave velocity structure in the upper mantle beneath Eurasia”, *Geophysical Journal International*, Vol. 174, pp. 978–992.
- Lienert, B. R., E. Berg and L. N. Frazer, 1986, “HYPOCENTER: An earthquake location method using centered, scaled, and adaptively damped least squares”, *Geological Society of America Bulletin*, Vol. 76, pp. 771-783.
- Lienert, 1991, “Report on modifications made to Hypocenter”, *Technical report*, Institute of Solid Earth Physics, University of Bergen, Bergen, Norway.
- Lienert, B. R. E. and J. Havskov, 1995, “A computer program for locating earthquakes both locally and globally”, *Seismological Research Letters*, Vol. 66, pp. 26-36.
- Makris, J., Z. Ben-Avraham, A. Behle, A. Ginzburg, P. Giesse, L. Steinmetz, R.B. Whitmarsh and S. Eleftheriou, 1983, “Seismic refraction profiles between Cyprus and Israel and their interpretation”, *The Geophysical Journal of the Royal Astronomical Society*, Vol. 75, pp. 575–591.
- McClusky, S., S. Balassanian, A. Barka, C. Demir, S. Ergintav, I. Georgiev, O. Gürkan, M. Hamburger, K. Hurst, H. Kahle, K. Kastens, G. Kekelidze, R. King, V. Kotzev, O. Lenk, S. Mahmoud, A. Mishin, M. Nadariya, A. Ouzounis, D. Paradissis, Y. Peter, M. Prilepin, R. Reilinger, I. Şanlı, H. Seeger, A. Tealeb, M. N. Toksöz and G. Veis, 2000, “Global Positioning System Constraints on Plate Kinematics and Dynamics in the Eastern Mediterranean and Caucasus”, *Journal of Geophysical Research*, Vol. 105, pp. 5695– 5719.

- McClusky, S., Reilinger, R., Mahmoud, S., Ben Sari, D. and A. Tealeb, 2003, “GPS constraints on Africa (Nubia) and Arabia plate motions”, *Geophysical Journal International*, Vol. 155, pp. 126–138.
- McKenzie, D. P., 1970, “Plate tectonics of the Mediterranean region”, *Nature*, Vol. 226, pp. 239-243.
- McKenzie, D. P., 1972, “Active Tectonics of the Mediterranean region”, *Royal Astronomical Society Geophysical Journal*, Vol. 30, pp. 109-185.
- McQuarrie, N., J. M. Stock., C. Verdel and B. P. Wernicke, 2003, “Cenozoic evolution of Neotethys and implications for the causes of plate motions”, *Geophysical Research Letters*, Vol. 30, pp. 2036.
- Moores E.M. and F. J. Vine, 1971, “The Troodos Massif, Cyprus and other Ophiolites as Oceanic Crust: Evaluation and Implications”, *Philosophical Transactions of the Royal Society of London. Series A, Mathematical and Physical Sciences*, Vol. 268, pp. 443-467.
- Mutlu, A.K. and H. Karabulut, 2011, “Anisotropic Pn tomography of Turkey and adjacent regions”, *Geophysical Journal International*, 187, pp. 1743–1758.
- Netzeband, G. L., K. Gohl, C.P. Hübscher, Z. Ben-Avraham, G.A. Dehghani, D. Gajewski and P. Liersch, 2006, “The Levantine Basin—crustal structure and origin”, *Tectonophysics*, Vol. 418, pp.167–188.
- Nur, A. and Z. Ben-Avraham, 1978, “The eastern Mediterranean and the Levant: tectonics of continental collision”, *Tectonophysics*, Vol. 46, pp. 297-311.
- Özel E., A. Uluğ and B. Pekçetinöz, 2007, “Neotectonic aspects of the northern margin of the Adana-Cilicia submarine basin, NE Mediterranean”, *Journal of Earth System Science*, Vol. 116, pp. 113-124.

- Pilidou, S., K. Priestley, J. Jackson and A. Maggi, 2004, “The 1996 Cyprus earthquake: a large, deep event in the Cyprean Arc”, *Geophysical Journal International*, Vol. 158, pp. 85–97.
- Piromallo, C., and A. Morelli, 2003, “P Wave Tomography of the Mantle Under the Alpine-Mediterranean Area”, *Journal of Geophysical Research*, Vol. 108 (B2), pp. 2065.
- Reilinger, R. S. McClusky, P. Vernant, S. Lawrence, S. Ergintav, R. Cakmak, H. Özener, F.Kadirov, I. Guliev, R. Stepanyan, M. Nadariya, G. Hahubia, S. Mahmoud, K. Sakr, A.ArRajehi, D. Paradissis, A. Al-Aydrus, M. Prilepin, T. Guseva, E. Evren, A. Dmitrotsa, S. V. Filikov, F. Gomez, R. Al-Ghazzi and G. Karam, 2006, “GPS constraints on continental deformation in the Africa–Arabia–Eurasia continental collision zone and implications for the dynamics of plate interactions”, *Journal of Geophysical Research*, Vol. 111, pp. V05411.
- Robertson, A.H.F., 1998, “Tectonic significance of the Eratosthenes Seamount: a continental fragment in the process of collision with subduction zone in the eastern Mediterranean”, *Tectonophysics*, Vol. 298, pp. 63–82.
- Robertson, A. H. F., 2000, “Mesozoic-Tertiary tectonic-sedimentary evolution of a South Tethyan oceanic basin and its margins in southern Turkey”, in Bozkurt, E., Winchester, J. A., and Piper, J. D. A., (eds.) *Tectonics and magmatism in Turkey and the surrounding area*, Geological Society of London, Vol. 173, pp. 97-138.
- Ryan, W.B.F., 1971, “Stratigraphy of Late Quaternary sediments in the eastern Mediterranean” In Stanley, D.J. (Ed.), *The Mediterranean Sea: A natural sedimentation laboratory*; Stroudsburg, (Dowden, Hutchinson and Ross), pp. 149-169.
- Salaün, G. H. A. Pedersen, A. Paul, V. Farra, H. Karabulut, D. Hatzfeld, C. Papazachos, D.M. Childs, C. Pequegnat and SIMBAAD Team, 2012, “High-resolution surface

- wave tomography of the Aegean-Anatolia region: constraints on upper mantle structure”, *Geophysical Journal International*, Vol. 190, pp. 406–420.
- Smith, A. G., 1971, “Alpine deformation and the oceanic areas of the Tethys, Mediterranean and Atlantic”, *Geological Society of America Bulletin.*, Vol. 82, pp. 2039-2070.
- Spakman, W. ,1991, “Delay-time tomography of the upper mantle below Europe, the Mediterranean, and Asia Minor”, *Geophysical Journal International*, Vol. 107, pp. 309–332.
- Şengör, A. M. C. and W. S. F. Kidd, 1979, “The post-collisional tectonics of the Turkish-Iranian Plateau and a comparison with Tibet”, *Tectonophysics*, Vol. 55, pp. 361-376.
- Şengör, A., M., C., N., Görür and F. Şaroğlu, 1985, “Strike-slip faulting and related basin formation in zones of tectonic escape: Turkey as a case study”, In: Biddle, K., and Christie-Blick, N., (eds), *Strike-slip Deformation, Basin Formation and Sedimentation, Society of Economic Paleontologists and Mineralogists, Special Publications*, Vol. 37, pp. 227-264.
- Şengör, A. M. C., S. Özeren, M. Keskin, M., Sakıncı, A. D. Özbakır and İ. Kayan, 2008, “Eastern Turkish high plateau as a small Turkic-type orogen: Implications for post-collisional crust-forming processes in Turkic-type orogens”, *Earth-Science Reviews*, Vol. 90, pp. 1-48.
- Tapponnier, P., G. Peltzer, A. Y. Le Dain, R. Armijo and P. Cobbold, 1982, “Propagating extrusion tectonics in Asia: New insight from simple experiments with plasticine”, *Geology*, Vol. 10, pp. 1339–1384.
- Tesauro M., M. K. Kaban, and S. A. P. L. Cloetingh, 2007, “EuCRUST-07: A new reference model for the European crust”, *Geophysical Research Letters*, Vol. 35, L05313.

- Vidal N., D. Klaeschen, D., A. Kopf, C. Docherty, R. Von Huene and V. A. Krasheninnikov, 2000, "Seismic images at the convergence zone from south of Cyprus to the Syrian coast, eastern Mediterranean", *Tectonophysics*, Vol. 329, pp. 157–170.
- Wdowinski S., Z. Ben-Avraham, R. Arvidsson and G. Ekström, 2006, "Seismotectonics of the Cyprian Arc", *Geophysical Journal International*, Vol. 164, pp. 176–181.
- Woodside, J.M., J. Mascle, T.A.C. Zitter, A. F. Limonov, M. Ergun and A. Volkonskaia, 2002, "The Florence Rise, the western bend of the Cyprus Arc", *Marine Geology*, Vol. 185, pp. 177–194.
- Wortel, R. and W. Spakman, 2000, "Subduction and Slab Detachment in the Mediterranean-Carpathian Region", *Science*, Vol. 290, pp. 1910-1917.